Robotics and Autonomous Systems 132 (2020) 103608

Contents lists available at ScienceDirect

Robotics and Autonomous Systems

journal homepage: www.elsevier.com/locate/robot

Range-based target localization and pursuit with autonomous vehicles: An approach using posterior CRLB and model predictive control☆

Nguyen T. Hung [a,*], N. Crasta [a], David Moreno-Salinas [b], António M. Pascoal [a], Tor A. Johansen [c]

[a] ISR/IST, University of Lisbon, Lisbon, Portugal
[b] Department of Computer Science and Automatic Control, National Distance Education University, Madrid, Spain
[c] Center for Autonomous Marine Operations and Systems (AMOS), Trondheim, Norway

ARTICLE INFO

Article history:
Received 28 February 2020
Received in revised form 27 June 2020
Accepted 20 July 2020
Available online 28 July 2020

Keywords:
Range-based target localization
Target tracking
Target pursuit
MPC
Fisher information matrix
Posterior CRLB
Autonomous vehicle

ABSTRACT

We address the general problem of multiple target localization and pursuit using measurements of the ranges from the targets to a set of autonomous pursuing vehicles, referred to as trackers. We develop a general framework for targets with models exhibiting uncertainty in the initial state, process, and measurement noise. The main objective is to compute optimal motions for the trackers that maximize the range-based information available for target localization and at the same time yield good target pursuit performance. The solution proposed is rooted in an estimation-theoretical setting that involves the computation of an appropriately defined Bayesian Fisher Information Matrix (FIM). The inverse of the latter yields a posterior Cramér–Rao Lower Bound (CRLB) on the covariance of the targets' state estimation errors that can be possibly achieved with any estimator. Using the FIM, sufficient conditions on the trackers' motions are derived for the ideal relative geometry between the trackers and the targets for which the range information acquired is maximal. This allows for an intuitive understanding of the types of ideal tracker trajectories. To deal with realistic constraints on the trackers' motions and the requirement that the trackers pursue the targets, we then propose a model predictive control (MPC) framework for optimal tracker motion generation with a view to maximizing the predicted range information for target localization while taking explicitly into account the trackers' dynamics, strict constraints on the trackers' states and inputs, and prior knowledge about the targets' states. The efficacy of the MPC is assessed in simulation through the help of representative examples motivated by operational scenarios involving single and multiple targets and trackers.

1. Introduction

The problem of target localization and pursuit has received widespread attention due to its importance in a vast number of applications in the areas of marine science, surveillance and reconnaissance, search-and-rescue, and military operations, see [1–4]. In the literature, *localization* usually refers to the problem of finding the location of an unknown stationary target, while tracking refers to the task of estimating the trajectory of a moving target. In the present paper, localization includes both tasks. *Pursuit*, in what follows, has the more control-oriented meaning of ensuring that in the course of their motion the entities in charge of estimating the trajectories of the targets stay in pre-defined neighborhoods of the targets. In this context, target pursuit is a secondary task that aims to enhance the "visibility" of the targets so as to yield better quality of the information available for target localization. In the present paper, this information consists of measurements of the ranges between the trackers and the targets.

The simplest and most classical problem of range-based target localization is that of computing the position of a single fixed target using a network of fixed sensors equipped with range-measuring devices. A fundamental problem arising in this context is that of deciding on the number of sensors and how to best place them so that the position of the target can be uniquely estimated with a desired level of accuracy (optimal sensor placement). A

☆ This research was supported in part by the H2020 EU Marine Robotics Research Infrastructure Network (ID: 731103), the FCT Projects: OceanTech (ID: POCI-01-0247-FEDER-024508), Mero (ID: CMUP-ERI/TIC/0045/2014), +Atlantic (ID: MERO/MITEXPL/ISF/0115/2017), LARSyS - FCT Project (ID: UIDB/50009/2020), and the Research Council of Norway (ID: 223254).

* Corresponding author.
E-mail addresses: hungnguyen@isr.ist.utl.pt (N.T. Hung), ncrasta@isr.ist.utl.pt (N. Crasta), dmoreno@dia.uned.es (D. Moreno-Salinas), antonio@isr.ist.utl.pt (A.M. Pascoal), tor.arne.johansen@itk.ntnu.no (T.A. Johansen).

https://doi.org/10.1016/j.robot.2020.103608
0921-8890/

solution to this problem can be obtained by adopting an estimation theoretical framework that involves the computation of an appropriately defined Fisher information matrix (FIM). See for example [5–7] for a discussion of these issues. See also [8] for optimal sensor placement solutions in the case of multiple static targets and sensors.

In recent years, there has been growing interest in exploiting the use of single or multiple mobile sensors (called trackers) for target localization, focusing on applications with unmanned aerial vehicles (UAVs) and autonomous marine vehicles (AMVs), see for example [1,9–13] and the references therein. In this setup, the trackers carry range measuring devices to acquire successive ranges to the targets of interest and use the range information to estimate the state of each target. Obviously, this approach has many advantages when compared with the traditional method of using a fixed sensor network. First, thanks to the mobility of the trackers, ranges can be acquired from a large number of positions relative to each target, thus potentially providing more information for target localization [9]. Second, the visibility of the targets can be facilitated by controlling the trackers to be close to the targets. In the marine environment the use of trackers in the form of AMVs avoids the cumbersome and costly deployment of long baseline (LBL) systems that are classically used in underwater target localization.

This, however leads to the challenging problem of how to plan the motion of the trackers such that their maneuvers ensure that the measured ranges from the trackers to the targets yield, in a well defined mathematical sense, the information needed to estimate the position of the target with a given level of accuracy through the use of an appropriately designed estimator. Technically, the answer to this problem should provide conditions on the motions of trackers that yield target motion observability, given measurements of the ranges between trackers and targets. A classical approach to this problem reported in the literature is to utilize tools from observability analysis, see for example [12, 14–17] and references therein. For instance, in [14], the author shows that it is impossible to observe a target moving at a constant velocity vector if the tracker (observer) moves at a constant velocity as well. However, if the tracker's trajectory is composed of at least two straight line segments with different orientations, the target's motion is observable if certain conditions on the bearing between the tracker and the target are satisfied. This analysis is further investigated in [15] where the trajectory of the tracker is considered to be smooth. In [16], the author analyzes the relative motion between the target and tracker using observability rank condition given in the work of [18]. Recent work in [17] provides a set of necessary and sufficient conditions on the motions of one or two trackers under which different type's of target's motions are observable. In general, the above approaches provide conditions on the tracker's trajectories that yield target state observability. However, these are essentially qualitative result that do not provide a good measure of how observable the target motions, a key requisite for adequate tracker motion planning.

A quantitative approach to motion planning can be derived using the celebrated Fisher Information Matrix (FIM), as a means to quantify the amount of information that range measurements carry about the motions of a target. Using this approach, the target localization problem is converted into that of finding conditions on the trackers' trajectories that maximize range-related information available to estimate the target's state. We recall that in an estimation theoretical framework, the inverse of the FIM yields a lower bound (the celebrated Cramér–Rao lower bound, abbreviated CRLB) on the covariance of the target's state estimation error that can possibly be achieved with any practical estimator [4,19,20]. In the context of range-based target localization, the CRLB is mostly used to access the performance that can be achieved with target state estimators [4,21]. A number of studies that exploit the use of the FIM for tracker motion planning have been published in the literature, see [9,13,22] and the reference therein for the case of one tracker one target. More recently, similar tools have been used to tackle the tracker motion planning problem in the case of multiple tracker–multiple target configurations [13]. Notice, however that in [13,22] the authors resort to the use of the so-called parametric FIM. In this context, the targets evolve in a deterministic manner and the initial conditions of the targets are viewed as parameters to be estimated. As such, the work eschews the far more realistic case where the initial state of the targets (prior information) is described by a random variable that captures the uncertainty in their location, a fact that mandates the use of so-called Bayesian FIM and the computation of posterior CRLBs [19], explained later in the present paper. Most approaches to target localization, including those reported in [13,22], also fail to address explicitly the constraints introduced by the limitations in the maneuverability of the trackers. In addition, the guidance law proposed in [13,22] for the trackers is based on the assumption that the motions of the targets are known in advance, which is unrealistic in the context of target localization. Still, the results in [13] are valuable in terms of understanding at an intuitive level, what kinds of optimal tracker trajectories are suited to selected types of target motion patterns.

Motivated by the above considerations, in the present paper we provide an answer to the question of "how to plan optimal motions" for a set of trackers so as to maximize the range information available to localize and pursue multiple unknown targets by exploiting the properties of an appropriately defined Bayesian FIM. Specifically, the main contributions of the paper include the following:

(i) We construct a Bayesian FIM using the range measurements from multiple trackers to multiple targets as a means to quantify the range information for the estimation of targets' states. The formalism adopted allows for the study of problems far more appropriate and realistic than those addressed in [13]. First, we consider a more general scenario (later denoted *Scenario B*) where the velocity vectors of the targets are considered to be unknown and must be estimated. Second, the motion of targets are considered to be a dynamical system with given prior information, allowing us to incorporate explicitly the prior knowledge of the targets' states. Third, the FIM in the current paper is the Bayesian FIM [19] which is more suitable and appropriate for the problem considered than the parametric FIM studied in [13]. The Bayesian FIM takes into account the dynamics of the trackers and the targets systematically and is computed sequentially, making its computation simpler, clean and more transparent than the method adopted in [13]. Fourth, the depths of the trackers and targets are explicitly taken into account. Lastly, we derive sufficient conditions on the relative geometry between the trackers and the targets trajectory under which the range information computed by the determinant of the FIM is maximum.

(ii) We also propose an MPC-based tracker motion planning, control, and estimation strategy that takes into account the trackers' constraints explicitly, in order to plan optimal motions for the trackers to localize and pursue the targets. In the MPC framework adopted, the control and planing processes are based on the estimated information about the target, thus making the approach more realistic than the guidance law given in [13] where the targets' motions are assumed to be known in advance.

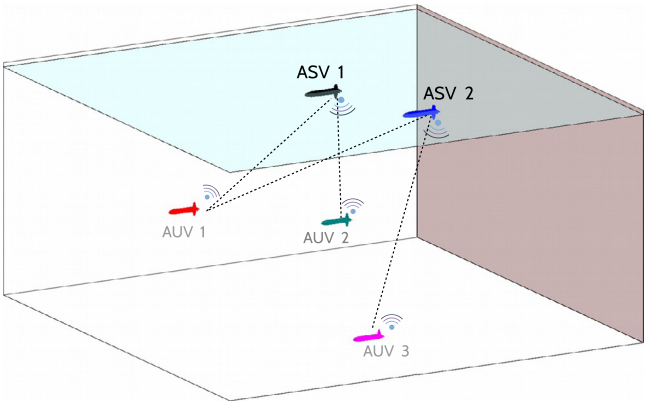

Fig. 3.1. An example of two trackers (ASVs) localizing three targets (AUVs) using acoustic range measurements.

The paper is organized as follows. Section 2 summarizes the basic notation. The general range-based multiple target localization and pursuit problem is formulated in Section 3. Section 4 describes the process of deriving an appropriate Bayesian FIM in the context of range-based target localization. Section 5 provides an analysis on the optimal motion of the trackers for the special case when the prior knowledge and the process noise are neglected. Section 6 presents an MPC-based method to solve the range-based target localization and pursuit problem in realistic contexts. Illustrative simulations are presented in Section 7. Section 8 contains the main conclusions.

2. Notation

We denote by I_n the identity matrix of size n and by $0_{m\times n}$ the zero matrix of size $m \times n$. For two matrices $A, B \in \mathbb{R}^{n\times n}$ the notation $A \succeq B$ implies that $A - B$ is a positive semi-definite matrix. We further let $\det(\cdot)$ and $\mathrm{Tr}(\cdot)$ denote the determinant and the trace of a square matrix, respectively. The symbol $\|\cdot\|$ denotes the Euclidean norm of a vector in $\mathbb{R}^n$. Given $\mathbf{x} \in \mathbb{R}^n$ and a symmetric positive-definite matrix $D \in \mathbb{R}^{n\times n}$, $\|\mathbf{x}\|_D^2 \triangleq \mathbf{x}^{\mathrm{T}} D\mathbf{x}$. Given a set of matrices $W_1, \ldots, W_p \in \mathbb{R}^{n\times m}$, the symbol $\mathrm{Diag}(W_1, \ldots, W_p)$ means the block diagonal matrix whose diagonal blocks are the matrices $W_k; k \in \{1, \ldots, p\}$. Given a set of vectors $\mathbf{x}_1, \ldots, \mathbf{x}_p$, $\mathrm{col}(\mathbf{x}_i) = [\mathbf{x}_1^{\mathrm{T}}, \ldots, \mathbf{x}_p^{\mathrm{T}}]^{\mathrm{T}}$.

3. Problem formulation

3.1. System model

Consider a group of trackers charged with the task of localizing and pursuing a group of moving targets whose motions are partially unknown. As an example, Fig. 3.1 illustrates the situation where two autonomous surface vehicles (ASVs) localize and pursue three autonomous underwater vehicles (AUVs) using acoustic range measurements. In general, given $p, q \in \mathbb{N}$, we define $\mathcal{S} \triangleq \{1, \ldots, p\}$ and $\mathcal{S}_{\mathrm{T}} \triangleq \{1, \ldots, q\}$, where p and q denote the number of trackers and targets, respectively. In what follows, $\{\mathcal{I}\} = \{x_{\mathcal{I}}, y_{\mathcal{I}}, z_{\mathcal{I}}\}$ denotes an inertial coordinate frame and $\{\mathcal{B}\}^{[i]} = \{x_{\mathcal{B}}^{[i]}, y_{\mathcal{B}}^{[i]}, z_{\mathcal{B}}^{[i]}\}$ denotes a body coordinate frame attached to tracker i; $i \in \mathcal{S}$. We now discuss the tracker and target models considered in this paper.

Tracker dynamics: For each $i \in \mathcal{S}$, let $z^{[i]}$ be the $z_{\mathcal{I}}$ coordinate of tracker i in frame $\{\mathcal{I}\}$. For the sake of simplicity, when analyzing the geometry of the motion of trackers, we assume that all trackers operate at known constant but possibly different depths, that is, $z^{[i]}(t) = \bar{z}^{[i]}$ for all $t \geq 0$ and $i \in S$. With the above assumptions,

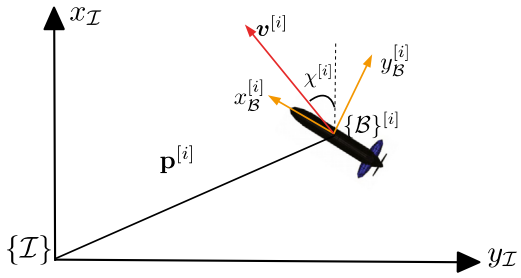

Fig. 3.2. Illustration of the planar motion of vehicle i.

the planar motion of tracker i; $i \in \mathcal{S}$, can be described by the simplified kinematic model

$$\dot{\mathbf{p}}^{[i]} = v^{[i]}[\cos(\chi^{[i]}), \sin(\chi^{[i]})]^{\mathrm{T}}, \quad \dot{\chi}^{[i]} = r^{[i]}, \tag{1}$$

where $\mathbf{p}^{[i]} = [x^{[i]}, y^{[i]}]^{\mathrm{T}} \in \mathbb{R}^2$ is the horizontal position of tracker i in $\{\mathcal{I}\}$; $v^{[i]} = \left\|\boldsymbol{v}^{[i]}\right\|$ is its total linear speed; $\chi^{[i]}$ is the course angle (see Fig. 3.2), and $r^{[i]}$ is the course angle rate. Notice that if the sideslip angle of the tracker is sufficiently small to be ignored, then course angle and course angle rate are equivalent to heading angle and yaw rate, respectively. Our main objective is to find *smooth* linear speed and course rate references for an autopilot to drive the trackers along trajectories that yield rich range-information for target localization. We introduce the following constraints

$$\dot{v}^{[i]} = a_v^{[i]}, \quad \dot{r}^{[i]} = a_r^{[i]}, \tag{2}$$

where $a_v^{[i]}$ and $a_r^{[i]}$ denote the linear and angular acceleration of the tracker, respectively, which we assume are bounded. In state-space form, we let $\mathbf{z}^{[i]} = [x^{[i]}, y^{[i]}, \psi^{[i]}, v^{[i]}, r^{[i]}]^{\mathrm{T}} \in \mathbb{R}^5$ be the state vector and $\mathbf{v}^{[i]} = [a_v^{[i]}, a_r^{[i]}]^{\mathrm{T}} \in \mathbb{R}^2$ the input vector. The tracker's model (1) can now be rewritten as

$$\begin{cases} \dot{\mathbf{z}}^{[i]} = \mathbf{g}(\mathbf{z}^{[i]}, \mathbf{v}^{[i]}), \\ \mathbf{p}^{[i]} = C\mathbf{z}^{[i]} \end{cases} \tag{3}$$

where $\mathbf{g}\colon \mathbb{R}^5 \times \mathbb{R}^2 \to \mathbb{R}^5$ and $C \in \mathbb{R}^{2\times 5}$ are given by

$$\mathbf{g}(\mathbf{z}^{[i]}, \mathbf{v}^{[i]}) = \begin{bmatrix} v^{[i]}\cos(\chi^{[i]}) \\ v^{[i]}\sin(\chi^{[i]}) \\ r^{[i]} \\ a_v^{[i]} \\ a_r^{[i]} \end{bmatrix} \quad \text{and} \quad C = \begin{bmatrix} I_2 & 0_{2\times 3} \end{bmatrix},$$

respectively. Later, for the purpose of system design, (3) will be discretized in time, yielding

$$\begin{cases} \mathbf{z}_{k+1}^{[i]} = \mathbf{g}_{\mathrm{d}}(\mathbf{z}_k^{[i]}, \mathbf{v}_k^{[i]}), \\ \mathbf{p}_k^{[i]} = C\mathbf{z}_k^{[i]}, \end{cases} \tag{4}$$

where $k \in \mathbb{N}$ indexes discrete time instants and $\mathbf{g}_{\mathrm{d}}(\cdot)$ is a nonlinear function that depends on the chosen discretization procedure. Due to physical limitations, the linear and the rotational speeds and the accelerations of the trackers are bounded. For this reason, we will impose the state and input constraints

$$\mathbf{v}^{[i]} \in \mathcal{V}^{[i]}, \quad \mathbf{z}^{[i]} \in \mathcal{Z}^{[i]}, \tag{5}$$

where $\mathcal{V}^{[i]} \subseteq \mathbb{R}^2$ and $\mathcal{Z}^{[i]} \subseteq \mathbb{R}^5$ are input and state constraint sets, respectively, for trackers i; $i \in \mathcal{S}$.

Target model: Let $z_{\mathrm{T}}^{[\alpha]}$ be the $z_{\mathcal{I}}$ coordinate of target α in $\{\mathcal{I}\}$. We assume that all targets move at known and constant depths, that is, $z_{\mathrm{T}}^{[\alpha]}(t) = \bar{z}_{\mathrm{T}}^{[\alpha]}$ for all $t \geq 0$ and $\alpha \in \mathcal{S}_{\mathrm{T}}$. Let also $\mathbf{q}_k^{[\alpha]} = [x_{\mathrm{T},k}^{[\alpha]}, y_{\mathrm{T},k}^{[\alpha]}]^{\mathrm{T}} \in \mathbb{R}^2$ be the projection of the target position vector

at discrete time k on the horizontal plane $x_{\mathcal{I}} - y_{\mathcal{I}}$. We consider each target α as a point mass whose motion is described by the discrete model

$$\mathbf{x}_{k+1}^{[\alpha]} = \mathbf{f}(\mathbf{x}_k^{[\alpha]}, \mathbf{u}_k^{[\alpha]}), \tag{6}$$

where $\mathbf{x}_k^{[\alpha]} \in \mathbb{R}^n$, $(n \geq 2)$ is the target's state vector that needs to be estimated, $\mathbf{u}_k^{[\alpha]} \in \mathbb{R}^2$ is the input vector. Note that $\mathbf{x}_k^{[\alpha]}$ includes $\mathbf{q}_k^{[\alpha]}$ and possibly $\dot{\mathbf{q}}_k^{[\alpha]}$. In this paper, we consider two instances of (6) corresponding to the following practical scenarios.

Scenario A: *Targets' velocity vectors are known*

To justify the assumption, consider a fleet of targets (AUVs) performing a pre-defined mission underwater, for example, cooperative path following [23], with known pre-defined velocity vectors. Under this assumption, we adopt the following target model:

Target model A

$$\mathbf{x}_{k+1}^{[\alpha]} = \mathbf{x}_k^{[\alpha]} + T_s \mathbf{u}_k^{[\alpha]}, \tag{7}$$

where $\mathbf{x}_k^{[\alpha]} = \mathbf{q}_k^{[\alpha]} \in \mathbb{R}^2$; $\mathbf{u}_k^{[\alpha]} \in \mathbb{R}^2$; $\alpha \in \mathcal{S}_{\mathrm{T}}$, is the target velocity vector in the inertial frame that is *known* to all the trackers; and $T_s > 0$ is the sampling interval. Consequently, in this particular case only the positions of the targets need to be estimated. We also assume that prior information on the initial target's state vector $\mathbf{x}_0^{[\alpha]}$ is given in terms of a Gaussian probability density function (PDF) described as

$$\mathbf{x}_0^{[\alpha]} \sim \mathcal{N}(\mathbf{c}_{\mathrm{A},0}^{[\alpha]}, P_{\mathrm{A},0}^{[\alpha]}) \tag{8}$$

with some $\mathbf{c}_{\mathrm{A},0}^{[\alpha]} \in \mathbb{R}^2$ and $P_{\mathrm{A},0}^{[\alpha]} \in \mathbb{R}^{2\times 2}$; $\alpha \in \mathcal{S}_{\mathrm{T}}$.

Scenario B: *Targets' velocity vectors are unknown*

In this case, the trackers need to estimate both the position and velocity vectors of each target. We also consider the case where the target's velocity vector changes slowly with time, so that it can be assumed to be approximately constant over the observation window, i.e. $\dot{\mathbf{q}}_k^{[\alpha]} = \mathbf{0}$ for all $\alpha \in \mathcal{S}_{\mathrm{T}}$. We thus let $\mathbf{x}_k^{[\alpha]} = [\mathbf{q}_k^{[\alpha]}; \dot{\mathbf{q}}_k^{[\alpha]}] \in \mathbb{R}^4$ be the state vector of the target α; $\alpha \in \mathcal{S}_{\mathrm{T}}$, that must be estimated. The following model for each target, named *Target model B*, can be rewritten explicitly from (6) as follows:

Target model B:

$$\mathbf{x}_{k+1}^{[\alpha]} = A_{\mathrm{B}} \mathbf{x}_k^{[\alpha]}, \tag{9}$$

where

$$A_{\mathrm{B}} = \begin{bmatrix} I_2 & T_s I_2 \\ 0_{2\times 2} & I_2 \end{bmatrix} \in \mathbb{R}^{4\times 4}. \tag{10}$$

Assume further that prior information on the initial target's state $\mathbf{x}_0^{[\alpha]}$ is given by the Gaussian PDF

$$\mathbf{x}_0^{[\alpha]} \sim \mathcal{N}(\mathbf{c}_{\mathrm{B},0}^{[\alpha]}, P_{\mathrm{B},0}^{[\alpha]}) \tag{11}$$

with some $\mathbf{c}_{\mathrm{B},0}^{[\alpha]} \in \mathbb{R}^4$ and $P_{\mathrm{B},0}^{[\alpha]} \in \mathbb{R}^{4\times 4}$; $\alpha \in \mathcal{S}_{\mathrm{T}}$.

Measurement model: We assume that each tracker is equipped with sensors that measure distances to all targets at the same discrete instants of time. At each time k, let $d_k^{[i,\alpha]}$ be the true distance from tracker i; $i \in \mathcal{S}$, to target α; $\alpha \in \mathcal{S}_{\mathrm{T}}$, defined as

$$d_k^{[i,\alpha]} = \sqrt{\left\|\mathbf{p}_k^{[i,\alpha]}\right\|^2 + \left(\bar{z}^{[i]} - \bar{z}_{\mathrm{T}}^{[\alpha]}\right)^2}, \tag{12}$$

where

$$\mathbf{p}_k^{[i,\alpha]} \triangleq \mathbf{p}_k^{[i]} - \mathbf{q}_k^{[\alpha]}. \tag{13}$$

Further, let $y_k^{[i,\alpha]}$ denote the range measurements which we assume are corrupted by Gaussian white noise according to the range measurement model

$$y_k^{[i,\alpha]} = d_k^{[i,\alpha]} + \eta_k^{[i,\alpha]}, \tag{14}$$

where $\eta_k^{[i,\alpha]} \sim \mathcal{N}(0, \sigma^2)$, $i \in \mathcal{S}$ and $\alpha \in \mathcal{S}_{\mathrm{T}}$. In practice, range measurements can only be obtained up to a certain distance that depends on the type of range-measuring device used and the environmental conditions (see [8]). Therefore, we make the following assumption.

Assumption 1. We assume that the farthest distance that can be measured reliably by any range-measuring devices is $d_{\max} > 0$. We further assume that all range measurements are taken within this distance, i.e. $d_k^{[i,\alpha]} \leq d_{\max}$ for all $k \in \mathbb{N}$, $i \in \mathcal{S}$ and $\alpha \in \mathcal{S}_{\mathrm{T}}$. These constraints will be addressed explicitly in Section 6.

3.2. Problem statement

The multiple target localization and pursuit problem can now be formally defined as follows.

Problem (*Target Localization and Pursuit*)**.** Consider a set of multiple trackers and a set of multiple targets. Assume the trackers' dynamics are given by (3) subject to input and state constraints (5), and the targets' model is given by (6) where the targets' states $\mathbf{x}_k^{[\alpha]}$; $\alpha \in \mathcal{S}_{\mathrm{T}}$ are unknown. Further assume that the range measurement model is given by (14). Under these conditions, design input $\mathbf{v}^{[i]}$; $i \in \mathcal{S}$ for each tracker so that the following tasks are fulfilled.

- Localization task: Ensure that the range measurements provide "sufficiently rich range information" to estimate the targets' states.
- Target pursuit: In addition to the localization task, guarantee that the trackers are in the vicinity of the targets, that is, ensure that the distance from any tracker to any target does not exceed $r^* \in (0, d_{\max}]$, where r^* is a design parameter.

A natural question that arises in this context is how to quantify the range information required to estimate the states of the targets with a desired level of accuracy. With this objective in mind we adopt an estimation theoretical setting that involves the computation of the FIM, whose definition and construction in the context of target localization are presented in the next section.

Remark 1. Notice that in the target localization and pursuit problem, target localization is the primary task while target pursuit is secondary. The objective of the latter is to keep the trackers close to the targets so as to acquire useful range measurements.

4. The Bayesian FIM in the context of range-based target localization

4.1. The Bayesian FIM for a general target model

We start by recalling the concept and construction of the Bayesian FIM that arises in the context of estimation of dynamical systems [19]. Consider the problem of estimating the state of a discrete nonlinear system described by

$$\begin{aligned} \mathbf{x}_{k+1} &= \mathbf{f}(\mathbf{x}_k, \mathbf{u}_k) + \mathbf{w}_k \\ \mathbf{y}_k &= \mathbf{h}(\mathbf{x}_k, \boldsymbol{\phi}_k) + \eta_k, \end{aligned} \tag{15}$$

where $\mathbf{x}_k \in \mathbb{R}^n$ is the state, $\mathbf{u}_k \in \mathbb{R}^m$ is a known deterministic input, $\mathbf{y}_k \in \mathbb{R}^l$ is the measurement output at discrete time k, $\boldsymbol{\phi}_k$ is a known deterministic trajectory (to be defined later) while $\mathbf{w}_k \sim \mathcal{N}(\mathbf{0}, Q)$ and $\eta_k \sim \mathcal{N}(\mathbf{0}, R)$ are independent Gaussian random processes that describe the state and measurement noises, respectively. In the context of range-based target localization, $\mathbf{h}(\cdot)$ are the distances from the trackers to the targets and $\boldsymbol{\phi}_k$ are the positions of the trackers (see (12)). Let $\hat{\mathbf{x}}_k$ be an estimator of $\mathbf{x}_k$ based on a set of k measurements samples $\{\mathbf{y}_i, \boldsymbol{\phi}_i, \mathbf{u}_{i-1}\}_{i=1}^k$ and the

prior knowledge of the initial probability density function $p(\mathbf{x}_0)$. According to [20], the covariance matrix of $\hat{\mathbf{x}}_k$, denoted P_k, given by any estimator is lower bounded as

$$P_k = \mathbb{E}\{(\hat{\mathbf{x}}_k - \mathbf{x}_k)(\hat{\mathbf{x}}_k - \mathbf{x}_k)^{\mathrm{T}}\} \succeq \mathcal{I}_k^{-1}, \tag{16}$$

where $\mathcal{I}_k$ is the so-called Fisher information matrix associated with the estimation of the state $\mathbf{x}_k$ and its inverse is the posterior CRLB. Applying the methodology described in [19], the Bayesian FIM is given by the recursive formula

$$\mathcal{I}_{k+1} = D_k^{22} - D_k^{21}(\mathcal{I}_k + D_k^{11})^{-1}D_k^{12}, \tag{17}$$

where

$$D_k^{11} = \mathbb{E}\Big\{ \left[\nabla_{\mathbf{x}_k}\mathbf{f}^{\mathrm{T}}(\mathbf{x}_k, \mathbf{u}_k)\right] Q^{-1} \left[\nabla_{\mathbf{x}_k}\mathbf{f}^{\mathrm{T}}(\mathbf{x}_k, \mathbf{u}_k)\right]^{\mathrm{T}} \Big\}, \tag{18}$$

$$D_k^{12} = -\mathbb{E}\big\{\nabla_{\mathbf{x}_k}\mathbf{f}(\mathbf{x}_k, \mathbf{u}_k)\big\}Q^{-1} = [D_k^{21}]^{\mathrm{T}}, \tag{19}$$

$$D_k^{22} = Q^{-1} + \Omega_{k+1}, \tag{20}$$

with

$$\Omega_{k+1} = \mathbb{E}\big\{H_{k+1}(\mathbf{x}_{k+1}, \boldsymbol{\phi}_{k+1})\big\} \tag{21}$$

and

$$\begin{aligned} &H_{k+1}(\mathbf{x}_{k+1}, \boldsymbol{\phi}_{k+1}) \\ &= \left[\nabla_{\mathbf{x}_{k+1}}\mathbf{h}^{\mathrm{T}}(\mathbf{x}_{k+1}, \boldsymbol{\phi}_{k+1})\right] R^{-1} \left[\nabla_{\mathbf{x}_{k+1}}\mathbf{h}^{\mathrm{T}}(\mathbf{x}_{k+1}, \boldsymbol{\phi}_{k+1})\right]^{\mathrm{T}}. \end{aligned} \tag{22}$$

In the above equations, $\mathbb{E}$ denotes the expectation operator and, for a given $\mathbf{x} = [x_1, \ldots, x_n]^{\mathrm{T}} \in \mathbb{R}^n$, $\nabla_{\mathbf{x}} \triangleq [\frac{\partial}{\partial x_1}, \ldots, \frac{\partial}{\partial x_n}]^{\mathrm{T}}$. Note that the expectation in (18) and (19) is with respect to the distribution of $\mathbf{x}_k$ while in (21) it is computed with respect to the distribution of $\mathbf{x}_{k+1}$. The recursion in (17) is initialized with the prior information of the initial state $\mathbf{x}_0$ as

$$\mathcal{I}_0 = \mathbb{E}\big\{[\nabla_{\mathbf{x}_0}\log p(\mathbf{x}_0)][\nabla_{\mathbf{x}_0}\log p(\mathbf{x}_0)]^{\mathrm{T}}\big\}. \tag{23}$$

We now consider a special case of (15) where the state equation is linear, given by

$$\begin{aligned} \mathbf{x}_{k+1} &= A\mathbf{x}_k + B\mathbf{u}_k + \mathbf{w}_k \\ \mathbf{y}_k &= \mathbf{h}(\mathbf{x}_k, \boldsymbol{\phi}_k) + \boldsymbol{\eta}_k. \end{aligned} \tag{24}$$

With this model, it follows from (18) and (19) that $D_k^{11} = A^{\mathrm{T}}Q^{-1}A$ and $D_k^{12} = A^{\mathrm{T}}Q^{-1}$. Inserting the later in (17) yields

$$\mathcal{I}_{k+1} = Q^{-1} + \Omega_{k+1} - Q^{-1}A(\mathcal{I}_k + A^{\mathrm{T}}Q^{-1}A)^{-1}A^{\mathrm{T}}Q^{-1}. \tag{25}$$

Applying the matrix inversion lemma,[1] (25) can be simplified as

$$\mathcal{I}_{k+1} = (Q + A\mathcal{I}_k^{-1}A^{\mathrm{T}})^{-1} + \Omega_{k+1}. \tag{26}$$

If A is non-singular and the process noise is absent, that is, if $Q = 0$ in (26), then

$$\mathcal{I}_{k+1} = [A^{-1}]^{\mathrm{T}}\mathcal{I}_k A^{-1} + \Omega_{k+1}. \tag{27}$$

Since $\mathbf{h}(\mathbf{x}_k, \boldsymbol{\phi}_k)$ is a nonlinear function of $\mathbf{x}_k$, in general it may be impossible to compute Ω_{k+1} given by (21) analytically. In practice, a Monte Carlo simulation method can be used to approximate the expectation operator. The key idea behind the Monte Carlo method is that, given $\mathbf{x}_0^{(j)} \sim p(\mathbf{x}_0); j = 1, \ldots, M$ and a sequence of $\{\mathbf{u}_i, \boldsymbol{\phi}_{i+1}\}_{i=0}^k$, we carry out M simulations of the system (24) to obtain M realizations of the trajectory $\{\mathbf{x}_{i+1}^{(j)}\}_{i=0}^k$. Then, the expectation in (21) can be computed approximately as

$$\Omega_{k+1} \approx \frac{1}{M}\sum_{j=1}^{M} H_{k+1}(\mathbf{x}_{k+1}^{(j)}, \boldsymbol{\phi}_{k+1}). \tag{28}$$

[1] $(A + BCD)^{-1} = A^{-1} - A^{-1}B(DA^{-1}B + C^{-1})^{-1}DA^{-1}$.

4.2. The Bayesian FIM for target model A

For each $i \in \mathcal{S}$, let $\mathcal{I}_{\mathrm{A},k}^{[i,\alpha]} \in \mathbb{R}^{2\times 2}$ be the Bayesian FIM at time k, associated with the estimation of the state $\mathbf{x}_k^{[\alpha]}$ of target α with motion described by *Target model A*, using the range measurements from tracker i. Notice that the system that results from the combination of *Target model A* given by (7) and the output model given by (12) is a special case of (24) with $A = I_2, B = T_s I_2, R = \sigma, \boldsymbol{\phi}_k = \mathbf{p}_k^{[i]}, Q = 0$ and $\mathbf{h}(\cdot) = d_k^{[i,\alpha]}$, where $d_k^{[i,\alpha]}$ is given by (12). Substituting the above parameters in (27), $\mathcal{I}_{\mathrm{A},k}^{[i,\alpha]}$ is given by

$$\mathcal{I}_{\mathrm{A},k+1}^{[i,\alpha]} = \mathcal{I}_{\mathrm{A},k}^{[i,\alpha]} + \Omega_{k+1}^{[i,\alpha]} \tag{29}$$

where $\Omega_{k+1}^{[i,\alpha]}$ is computed as in (21), yielding

$$\Omega_{k+1}^{[i,\alpha]} = \mathbb{E}\left\{\frac{1}{\sigma^2}\left(\frac{\mathbf{p}_{k+1}^{[i,\alpha]}}{d_{k+1}^{[i,\alpha]}}\right)\left(\frac{\mathbf{p}_{k+1}^{[i,\alpha]}}{d_{k+1}^{[i,\alpha]}}\right)^{\mathrm{T}}\right\} \tag{30}$$

with $\mathbf{p}_k^{[i,\alpha]}$ is given in (13). Note that the expectation in (30) is taken over the distribution of $\mathbf{q}_{k+1}^{[\alpha]}$. We now consider $\mathcal{I}_{\mathrm{A},k}^{[\alpha]}$, the FIM for estimating $\mathbf{x}_k^{[\alpha]}$, using the range measurements from all trackers, collectively. Compared with the case of a single tracker, more range measurements are augmented to the measurement output vector, i.e. $\mathbf{h}(\cdot) = [d_k^{[1,\alpha]}, \ldots, d_k^{[p,\alpha]}]^{\mathrm{T}} \in \mathbb{R}^p$ and $R = \mathrm{Diag}(\sigma, \ldots, \sigma) \in \mathbb{R}^{p\times p}$. Inserting the above in (27) yields

$$\mathcal{I}_{\mathrm{A},k+1}^{[\alpha]} = \mathcal{I}_{\mathrm{A},k}^{[\alpha]} + \sum_{i=1}^{p}\Omega_{k+1}^{[i,\alpha]}. \tag{31}$$

It follows from (8) and (23) that the recursions (29) and (31) start with the prior information

$$\mathcal{I}_{\mathrm{A},0}^{[i,\alpha]} = \mathcal{I}_{\mathrm{A},0}^{[\alpha]} = [P_{\mathrm{A},0}^{[\alpha]}]^{-1}, \tag{32}$$

that is, the FIM iterations start with the prior information on the target's positions. Let $\mathbf{x}_k = [\mathbf{x}_k^{[1]}, \ldots, \mathbf{x}_k^{[q]}] \in \mathbb{R}^{2q}$ be the states of all targets that need to be estimated. Also, let $\mathcal{I}_{\mathrm{A},k} \in \mathbb{R}^{2q\times 2q}$ denote the total information available to estimate $\mathbf{x}_k$ using all range measurements from all the trackers to each of the targets. Using the methodology mentioned in the previous cases it can be shown that

$$\mathcal{I}_{\mathrm{A},k} = \mathrm{Diag}(\mathcal{I}_{\mathrm{A},k}^{[1]}, \ldots, \mathcal{I}_{\mathrm{A},k}^{[q]}), \tag{33}$$

where each $\mathcal{I}_{\mathrm{A},k}^{[\alpha]}; \alpha = 1, \ldots, q$ is computed using (31).

4.3. The Bayesian FIM for target model B

For every $i \in \mathcal{S}$, let $\mathcal{I}_{\mathrm{B},k}^{[i,\alpha]} \in \mathbb{R}^{4\times 4}$ be the FIM associated with the estimation of the state $\mathbf{x}_k^{[\alpha]} \in \mathbb{R}^4$ of target α, with motion described by *Target model B*, using the range measurements from tracker i. Notice that *Target model B* given by (9) is a special case of (24) with $A = A_{\mathrm{B}}$, where A_{B} is given by (10), $R = \sigma, \boldsymbol{\phi}_k = \mathbf{p}_k^{[i]}, Q = 0$ and $\mathbf{h}(\cdot) = d_k^{[i,\alpha]}$. Substituting the above parameters in (27), $\mathcal{I}_{\mathrm{B},k}^{[i,\alpha]}$ is given by

$$\mathcal{I}_{\mathrm{B},k+1}^{[i,\alpha]} = [A_{\mathrm{B}}^{-1}]^{\mathrm{T}}\mathcal{I}_{\mathrm{B},k}^{[i,\alpha]}A_{\mathrm{B}}^{-1} + \begin{bmatrix}\Omega_{k+1}^{[i,\alpha]} & 0_{2\times 2}\\ 0_{2\times 2} & 0_{2\times 2}\end{bmatrix}. \tag{34}$$

Let $\mathcal{I}_k^{[\alpha]}$ be the FIM associated with the estimation of $\mathbf{x}_k^{[\alpha]}$ using the range measurements from all trackers, collectively. Similar to the case of *Target model A*, $\mathcal{I}_{\mathrm{B},k}^{[\alpha]}$ can be computed by the recursion formula

$$\mathcal{I}_{\mathrm{B},k+1}^{[\alpha]} = [A_{\mathrm{B}}^{-1}]^{\mathrm{T}}\mathcal{I}_{\mathrm{B},k}^{[\alpha]}A_{\mathrm{B}}^{-1} + \sum_{i=1}^{p}\begin{bmatrix}\Omega_{k+1}^{[i,\alpha]} & 0_{2\times 2}\\ 0_{2\times 2} & 0_{2\times 2}\end{bmatrix}. \tag{35}$$

It follows from (11) and (23) that the recursions (34) and (35) start with the prior information

$$\mathcal{I}_{\mathrm{B},0}^{[i,\alpha]} = \mathcal{I}_{\mathrm{B},0}^{[\alpha]} = [P_{\mathrm{B},0}^{[\alpha]}]^{-1}. \tag{36}$$

Let $\mathbf{x}_k = [\mathbf{x}_k^{[1]}, \ldots, \mathbf{x}_k^{[q]}]^{\mathrm{T}} \in \mathbb{R}^{4q}$ be the state of all targets that needs to be estimated. Also, let $\mathcal{I}_{\mathrm{B},k} \in \mathbb{R}^{4q\times 4q}$ denote the total information for estimating $\mathbf{x}_k$. Clearly, $\mathcal{I}_{\mathrm{B},k}$ is given by

$$\mathcal{I}_{\mathrm{B},k} = \mathrm{Diag}(\mathcal{I}_{\mathrm{B},k}^{[1]}, \ldots, \mathcal{I}_{\mathrm{B},k}^{[q]}), \tag{37}$$

where each $\mathcal{I}_{\mathrm{B},k}^{[\alpha]}; \alpha \in \mathcal{S}_{\mathrm{T}}$ is computed by (35).

Note that by construction, the FIM is symmetric and positive semi-definite. In the context of the present paper, the information carried by the FIM for estimation purposes is measured by its determinant, the metric adopted in [6,7].

5. Preliminary analysis: ideal geometries for maximum range-related information

In this section, we will analyze a special case of the Bayesian FIMs derived for *Target Model A* and *B* where *there is no prior information on the initial state of the target.*[2] We will show that this special case leads to simplified FIMs that allows us to derive analytically "ideal" condition on the trackers' trajectories that yield maximum achievable range-information acquired to estimate the targets' states. The results in this section helps understand at a very intuitive level the types of optimal relative tracker–target geometries that the trackers should reach and maintain to maximize the range-related information. Furthermore, they play an important role in benchmarking the types of solutions that will be obtained numerically using the far more realistic approach to target localization and pursuit introduced in Section 6.

To analyze the Bayesian FIMs with the above assumptions, their formulas in recursions (31) and (35) can be rewritten in compact form as follows. Firstly, let

$$a_n^{[i,\alpha]} = \left(x_n^{[i]} - x_{\mathrm{T},n}^{[\alpha]}\right)/d_n^{[i,\alpha]} \tag{38a}$$

$$b_n^{[i,\alpha]} = \left(y_n^{[i]} - y_{\mathrm{T},n}^{[\alpha]}\right)/d_n^{[i,\alpha]}, \tag{38b}$$

for all $n \in \{1, \ldots, k\}$. Define also two vectors $\mathbf{a}_{i,\alpha} = [a_1^{[i,\alpha]}, \ldots, a_k^{[i,\alpha]}]^{\mathrm{T}} \in \mathbb{R}^k$ and $\mathbf{b}_{i,\alpha} = [b_1^{[i,\alpha]}, \ldots, b_k^{[i,\alpha]}]^{\mathrm{T}} \in \mathbb{R}^k$.

Lemma 1. *Consider the Bayesian FIMs related to the problem of estimating the state of target α computed by recursions (31) and (35), corresponding to Target model A and Target model B, respectively. If there is no prior information on the initial target state, i.e. $\mathcal{I}_{\mathrm{A},0}^{[i,\alpha]} = 0_{2\times 2}$ in (32) and $\mathcal{I}_{\mathrm{B},0}^{[i,\alpha]} = 0_{4\times 4}$ in (36) then,*

$$\mathcal{I}_{\mathrm{A},k}^{[\alpha]} = \sum_{i=1}^{p} \frac{1}{\sigma^2} \begin{bmatrix} \|\mathbf{a}_{i,\alpha}\|^2 & \mathbf{a}_{i,\alpha}^{\mathrm{T}}\mathbf{b}_{i,\alpha} \\ \mathbf{a}_{i,\alpha}^{\mathrm{T}}\mathbf{b}_{i,\alpha} & \|\mathbf{b}_{i,\alpha}\|^2 \end{bmatrix} \tag{39}$$

and

$$\mathcal{I}_{\mathrm{B},k}^{[\alpha]} = \begin{bmatrix} A_\alpha & B_\alpha \\ B_\alpha & C_\alpha \end{bmatrix}, \tag{40}$$

where $A_\alpha = \mathcal{I}_{\mathrm{A},k}^{[\alpha]}$ with $\mathcal{I}_{\mathrm{A},k}^{[\alpha]}$ given by (39),

$$\begin{aligned} B_\alpha &= -\sum_{i=1}^{p} \frac{1}{\sigma^2} \begin{bmatrix} \|\mathbf{a}_{i,\alpha}\|_{D_1}^2 & \mathbf{a}_{i,\alpha}^{\mathrm{T}} D_1 \mathbf{b}_{i,\alpha} \\ \mathbf{a}_{i,\alpha}^{\mathrm{T}} D_1 \mathbf{b}_{i,\alpha} & \|\mathbf{b}_{i,\alpha}\|_{D_1}^2 \end{bmatrix}, \\ C_\alpha &= \sum_{i=1}^{p} \frac{1}{\sigma^2} \begin{bmatrix} \|\mathbf{a}_{i,\alpha}\|_{D_2}^2 & \mathbf{a}_{i,\alpha}^{\mathrm{T}} D_2 \mathbf{b}_{i,\alpha} \\ \mathbf{a}_{i,\alpha}^{\mathrm{T}} D_2 \mathbf{b}_{i,\alpha} & \|\mathbf{b}_{i,\alpha}\|_{D_2}^2 \end{bmatrix}, \end{aligned} \tag{41}$$

[2] Equivalent with $\mathcal{I}_{\mathrm{A},0}^{[i,\alpha]}$ in (32), $\mathcal{I}_{\mathrm{B},0}^{[i,\alpha]}$ in (36) are zero.

$D_1 = \mathit{Diag}(\tau_1, \ldots, \tau_k) \in \mathbb{R}^{k\times k}$, $D_2 = \mathit{Diag}(\tau_1^2, \ldots, \tau_k^2) \in \mathbb{R}^{k\times k}$ *and* $\tau_n = (k-n)T_{\mathrm{s}},\ n = \{1, \ldots, k\}$.

Proof. For *Target model A*, (39) is obtained by substituting $\mathcal{I}_{\mathrm{A},0}^{[i,\alpha]} = 0$ and the relation in (38) in (31), while for *Target model B*, (40) is obtained by substituting $\mathcal{I}_{\mathrm{B},0}^{[i,\alpha]} = 0$ and the relation in (38) in (35). Notice also that since the process noise is zero the target moves in a deterministic manner, thus, the expectation in (30) was dropped to obtain (39) and (40). ■

Before we proceed we introduce the variables

$$c^{[i,\alpha]} = \left(\frac{(\bar{z}^{[i]} - \bar{z}_{\mathrm{T}}^{[\alpha]})}{d_{\max}}\right)^2 \tag{42}$$

and $\gamma^{[i,\alpha]}$, with the latter defined by

$$\cos(\gamma_n^{[i,\alpha]}) = \frac{x_n^{[i]} - x_{\mathrm{T},n}^{[\alpha]}}{\left\|\mathbf{p}_n^{[i,\alpha]}\right\|} \tag{43}$$

for all $n \in \{1, \ldots, k\}$. By definition, $\gamma_n^{[i,\alpha]}$ is the angle between the projection on the $x_{\mathcal{I}} - y_{\mathcal{I}}$ plane of the relative position vector from tracker i to target α and the $x_{\mathcal{I}}$-axis (see Fig. 5.1). The main results in this section are presented next.

5.1. Single tracker-single target

We start by considering the simple case of a single tracker localizing a single target. In this configuration, $i = p = 1$ and $\alpha = q = 1$. Therefore, for simplicity of notation we drop the superscripts (subscripts) i and α wherever they appear in this subsection. The following result provides a measure of the range-related information available in this scenario.

Theorem 1. *Consider the case of a single tracker localizing a single target. Let assumptions in Lemma 1 hold. Then, the following statements hold true.*

i. For Scenario A, the range information quantified by $\det(\mathcal{I}_{\mathrm{A},k})$ *is maximal when* $\mathcal{I}_{\mathrm{A},k} = \mathcal{I}_{11\mathrm{A}}$, *where*

$$\mathcal{I}_{11\mathrm{A}} = (1-c)\sigma^{-2}\mathcal{I}_{\mathrm{A}}^{o}, \tag{44}$$

c is given by (42), and

$$\mathcal{I}_{\mathrm{A}}^{o} = kI_2/2. \tag{45}$$

ii. For Scenario B, $\det(\mathcal{I}_{\mathrm{B},k})$ *is maximal when* $\mathcal{I}_{\mathrm{B},k} = \mathcal{I}_{11\mathrm{B}}$, *where*

$$\mathcal{I}_{11\mathrm{B}} = (1-c)\sigma^{-2}\mathcal{I}_{\mathrm{B}}^{o}, \tag{46}$$

c is given by (42),

$$\mathcal{I}_{\mathrm{B}}^{o} = \begin{bmatrix} kI_2/2 & \Delta_1 I_2/2 \\ \Delta_1 I_2/2 & \Delta_2 I_2/2 \end{bmatrix}, \tag{47}$$

with $\Delta_1 \triangleq -\sum_{n=1}^{k}\tau_n$, and $\Delta_2 \triangleq \sum_{n=1}^{k}\tau_n^2$.

The matrices $\mathcal{I}_{11\mathrm{A}}$ and $\mathcal{I}_{11\mathrm{B}}$ are called the optimal range information matrices for Scenarios A and B, respectively.

Proof. See Appendix A.

Remark 2. For *Target model A*, if the tracker and the target are at the same depth, that is, $c = 0$, then the optimal FIM in (44) recovers the result in [13] (see Lemma 2 in [13] for the case one tracker-one target). This happens because, for this particular case, we assumed that there is no prior information

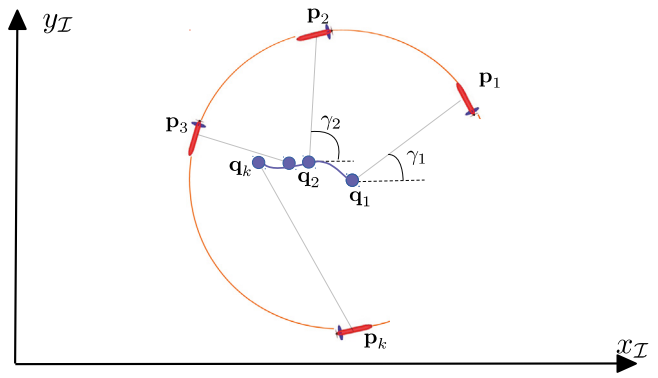

Fig. 5.1. One tracker-one target. An example of an ideal tracker–target geometry that maximizes the range information. Successive positions and respective trajectories of target (blue) and tracker (red). (For interpretation of the references to color in this figure legend, the reader is referred to the web version of this article.)

on the initial state of the target therefore, the target can be viewed as a deterministic process with unknown initial target's state. Thus, under these assumptions the simplified Bayesian FIM associated with the estimation of the target state at current time ($\mathbf{x}_k$) in the present paper is equivalent to the parametric FIM associated with the estimation of the initial target's state ($\mathbf{x}_0$) in [13]. However, it is important to stress that the parametric FIM in [13] is only applicable to deterministic target, whereas as shown in the previous section the Bayesian FIM is applicable to all types of target motion. Furthermore, the method used to compute the Bayesian FIM in the present paper is a recursive approach, which is simpler and more transparent than that used to compute the parametric FIM in [13].

We now study possible target–tracker geometries that maximize the range-related information. We obtain the following result.

Proposition 1. *Consider the case of a single tracker localizing a single target. In order to reach the maximal range information, as characterized in Theorem 1, an optimal trajectory for the tracker is obtained by encircling the projection of the target on the $x_{\mathcal{I}} - y_{\mathcal{I}}$ plane such that any two successive range measurements are taken at positions that satisfy*

$$\gamma_{n+1} - \gamma_n = \omega \triangleq \pm 2\pi/N \tag{48}$$

for all $n \in \{1, \ldots, k\}$, where γ_n defined in (43) and some $N \in \mathbb{N}$; $N \geq 3$. Furthermore, if the tracker and the target are at different depths, in addition to (48) the tracker encircles the target along a circumference of radius $r \triangleq \sqrt{d_{\max}^2 - (\bar{z} - \bar{z}_{\mathrm{T}})^2}$.

Proof. See Appendix A.

In (48), the symbol $\pm$ indicate the direction of the tracker's motion ("+" is counter-clockwise and "−" is clockwise). Proposition 1 implies that if the target is fixed (stationary), an ideal trajectory for the tracker is obtained by having the tracker follow a circumference centered at the target with a constant linear speed and a constant course rate, see Fig. 5.1.

5.2. Multiple trackers–single target

We now consider the case when more than one tracker is used to localize a single moving target and derive the following result.

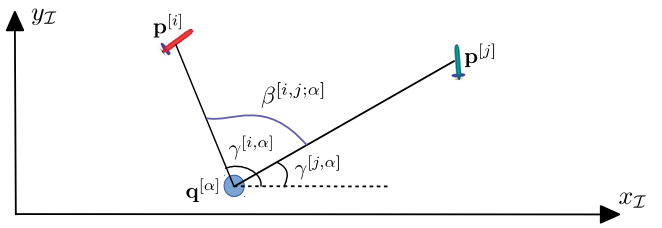

Fig. 5.2. Angle formed by the relative position vectors between trackers and target α in the $x_{\mathcal{I}} - y_{\mathcal{I}}$ plane.

Theorem 2. *Consider the case of p trackers localizing a single target, say α. Let assumptions in Lemma 1 hold. Then, the following statements hold true.*

i. For Scenario A, $\det(\mathcal{I}_{\mathrm{A},k}^{[\alpha]})$ is maximal when $\mathcal{I}_{\mathrm{A},k}^{[\alpha]} = \bar{\mathcal{I}}_{\mathrm{A},k}^{[\alpha]}$, where

$$\bar{\mathcal{I}}_{\mathrm{A},k}^{[\alpha]} = \left(p - \sum_{i=1}^{p} c^{[i,\alpha]}\right) \sigma^{-2} \mathcal{I}_{\mathrm{A}}^{o}, \tag{49}$$

$c^{[i,\alpha]}$ is given by (42), and $\mathcal{I}_{\mathrm{A}}^{o}$ is given by (45).

ii. For Scenario B, $\det(\mathcal{I}_{\mathrm{B},k}^{[\alpha]})$ is maximal when $\mathcal{I}_{\mathrm{B},k}^{[\alpha]} = \bar{\mathcal{I}}_{\mathrm{B},k}^{[\alpha]}$, where

$$\bar{\mathcal{I}}_{\mathrm{B},k}^{[\alpha]} = \left(p - \sum_{i=1}^{p} c^{[i,\alpha]}\right) \sigma^{-2} \mathcal{I}_{\mathrm{B}}^{o}, \tag{50}$$

$c^{[i,\alpha]}$ is given by (42), and $\mathcal{I}_{\mathrm{B}}^{o}$ is given in (47).

Proof. See Appendix A.

We now discuss possible geometries that maximize the range information. To this end, we shall study the angle $\beta^{[i,j;\alpha]}$ formed by the two relative position vectors from the trackers i and j to the target α in the $x_{\mathcal{I}} - y_{\mathcal{I}}$ plane (see Fig. 5.2). We obtain the following results.

5.2.1. Geometry for two trackers- single target ($p = 2$, $q = 1$)

Proposition 2. *Consider the case of two trackers localizing a single target α. In order to obtain maximal range information, as characterized in Theorem 2, an ideal trajectory for the trackers is to maintain the relative position vectors from the two trackers to the target orthogonal, that is,*

$$\beta_n^{[1,2;\alpha]} = \pi/2 + l\pi \tag{51}$$

for all $n \in \{1, \ldots, k\}$ and $l \in \mathbb{N}$. Furthermore, if the trackers and the target are at different depths, in addition to the orthogonality condition above the condition given by $\left\|\mathbf{p}_n^{[i]} - \mathbf{q}_n^{[\alpha]}\right\| = \sqrt{d_{\max}^2 - (\bar{z}^{[i]} - \bar{z}_{\mathrm{T}}^{[\alpha]})^2}$ for all $i \in \{1, 2\}$ and $n \in \{1, \ldots, k\}$ applies.

Proof. See Appendix A.

Fig. 5.3 illustrates possible trackers–target trajectories that maximize the range information when the trackers and the targets are at the same depth.

5.2.2. Geometry for multiple trackers - single target ($p \geq 3$, $q = 1$)

Proposition 3. *Consider the case of p trackers localizing a single target α. In order to obtain maximal range information, as characterized in Theorem 2, an ideal trajectory for the trackers is to keep them around the target in such a way that*

$$\beta_n^{[i,j;\alpha]} = \beta_n^{[j,i;\alpha]} = 2\pi/p \tag{52}$$

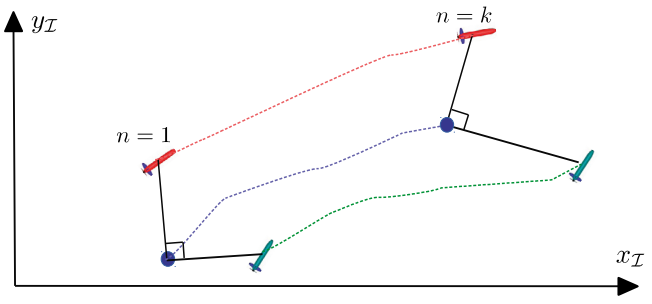

Fig. 5.3. Two trackers-one target. An example of ideal trackers–target trajectories that maximizes the range information. Tracker 1 (red), tracker 2 (green), target (blue). (For interpretation of the references to color in this figure legend, the reader is referred to the web version of this article.)

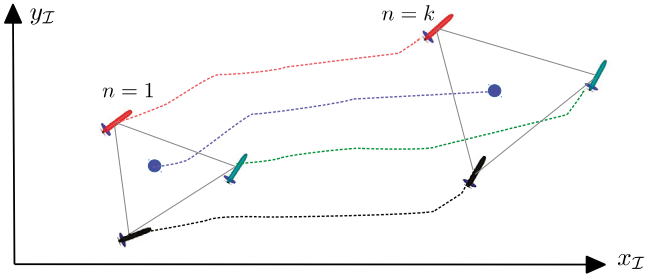

Fig. 5.4. Three trackers-one target. An example of ideal trackers–target trajectories that maximizes the range information. Tracker 1 (red), tracker 2 (green), tracker 3 (black), and target (blue). (For interpretation of the references to color in this figure legend, the reader is referred to the web version of this article.)

for all $i, j \in \mathcal{S}$ and $n \in \{1, \ldots, k\}$. Furthermore, if the trackers and the target are at different depths, in addition to the condition in (52) the condition given by $\left\|\mathbf{p}_n^{[i]} - \mathbf{q}_n^{[\alpha]}\right\| = \sqrt{d_{\max}^2 - (\bar{z}^{[i]} - \bar{z}_{\mathrm{T}}^{[\alpha]})^2}$ for all $n \in \{1, \ldots, k\}$ and $i \in \{1, \ldots, p\}$ applies.

Proof. See Appendix A.

Fig. 5.4 illustrates, for the case of three trackers and one target, possible tracker–target trajectories that yield the maximum range information when all trackers and the target are at the same depth. In this case, the trackers move in such a way as to keep the target at the in-center of the equilateral triangle formed by their positions, viewed as vertices of the triangle.

5.3. Multiple trackers–multiple targets ($p \geq 2, q \geq 2$)

We now consider the case of multiple trackers and multiple targets. We first characterize the optimal range-related FIM, as follows.

Theorem 3. *Consider the situation of p trackers localizing q targets. Let assumptions in Lemma 1 hold. Then, the following statements hold true.*

i. For Scenario A, $\det(\mathcal{I}_{\mathrm{A},k})$ is maximal when $\mathcal{I}_{\mathrm{A},k} = \bar{\mathcal{I}}_{\mathrm{A},k}$, where

$$\bar{\mathcal{I}}_{\mathrm{A},k} = \mathrm{Diag}(\bar{\mathcal{I}}_{\mathrm{A},k}^{[1]}, \ldots, \bar{\mathcal{I}}_{\mathrm{A},k}^{[q]}), \tag{53}$$

$\bar{\mathcal{I}}_{\mathrm{A},k}^{[\alpha]}$: $\alpha = \mathcal{S}_{\mathrm{T}}$ given by (49).

ii. For Scenario B, $\det(\mathcal{I}_{\mathrm{B},k})$ is maximal when $\mathcal{I}_{\mathrm{B},k} = \bar{\mathcal{I}}_{\mathrm{B},k}$, where

$$\bar{\mathcal{I}}_{\mathrm{B},k} = \mathrm{Diag}(\bar{\mathcal{I}}_{\mathrm{B},k}^{[1]}, \ldots, \bar{\mathcal{I}}_{\mathrm{B},k}^{[q]}), \tag{54}$$

$\bar{\mathcal{I}}_{\mathrm{B},k}^{[\alpha]}$: $\alpha = \mathcal{S}_{\mathrm{T}}$ given by (50).

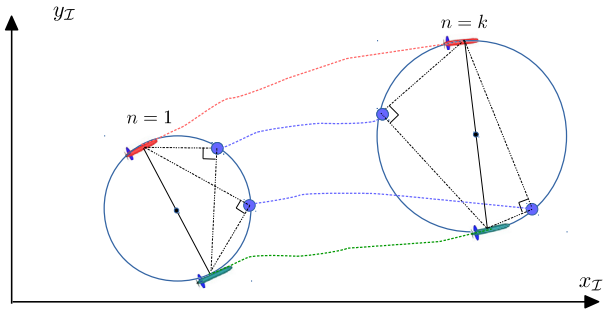

Fig. 5.5. Two trackers-two targets. An example of ideal trackers–targets trajectories that maximizes the range information. Targets trajectories (blue). Tracker 1 (red), tracker 2 (green). (For interpretation of the references to color in this figure legend, the reader is referred to the web version of this article.)

Proof. See Appendix A.

We now discuss the ideal geometry for the case of two trackers localizing multiple targets.

Proposition 4. *Consider the case of two trackers localizing q targets. In order to obtain maximal range information, as characterized in Theorem 3, ideal trajectories for the trackers correspond to maintaining the relative position vectors from them to each target orthogonal. Furthermore, if the trackers and the targets are at different depths, in addition to the orthogonality condition the condition given by $\left\|\mathbf{p}_n^{[i]} - \mathbf{q}_n^{[\alpha]}\right\| = \sqrt{d_{\max}^2 - (\bar{z}^{[i]} - \bar{z}_{\mathrm{T}}^{[\alpha]})^2}$ for all $n \in \{1, \ldots, k\}$, $i \in \{1, 2\}$ and $\alpha \in \mathcal{S}_{\mathrm{T}}$ applies.*

Proof. The proof is similar to that of Proposition 2. ■

Fig. 5.5 illustrates a possible tracker–target trajectory that maximizes the range information for the case of two trackers and two targets. It can be seen that, in order to obtain maximal range information, the trackers move so that the circumscribed circumference that is centered at the middle of the two trackers goes through the positions the targets.

6. MPC framework for target localization and pursuit

The previous section addressed the problem of multiple target localization using multiple trackers by characterizing the types of possible target–tracker geometries that yield maximum range-based information. The results obtained characterizes the ideal positions of the trackers with respect to the foreseen motion of the targets. The analysis provided valuable insight into the types of ideal tracker trajectories required. However, further work is required to bring these theoretical advances to bear on the development of effective target localization and pursuit systems. In fact, the analysis eschewed four key issues that occur in real situations: (i) the target's motion cannot be known completely in advance, (ii) the motions of the trackers may be severely restricted due to their dynamics and state/input constraints, (iii) the trackers should maneuver in the vicinity of the targets in order to ensure that range measurements can be obtained using appropriate acoustic sensors, and (iv) the optimal target–tracker geometries must be defined with respect to the estimated positions of the targets (obtained with a properly designed estimator), since the real states of the latter are unknown.

To address the above challenges, we propose a scheme that involves the execution of three different phases: optimal tracker motion planning based on prior information about the targets, motion control of the trackers based on the planned motion, and range-based target state estimation. To implement the first two,

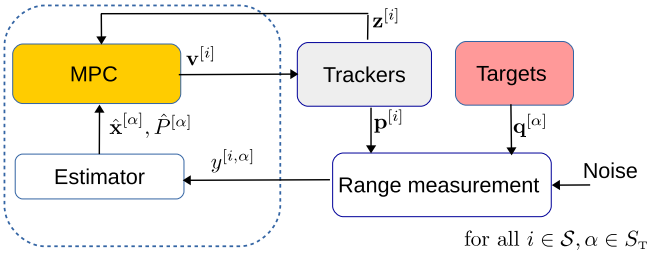

Fig. 6.1. Receding horizon strategy for target localization and pursuit.

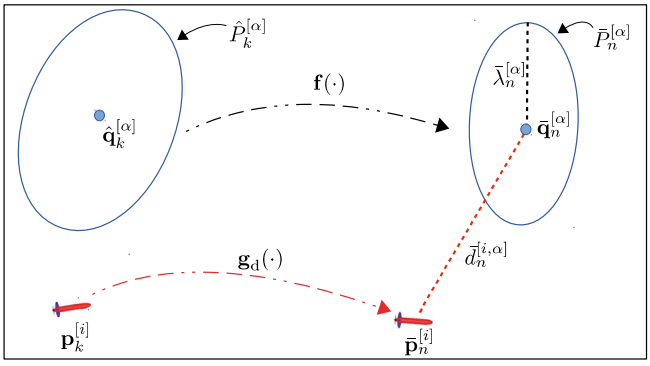

Fig. 6.2. Illustration of the predicted uncertainty of the target's position for *Target model A*. Recall that in this case the target's state only contains the target's position.

an MPC-like framework is adopted whereby the motions of the trackers are planned by resorting to a receding horizon framework. In this set-up, the cost criterion adopted includes in its structure a measure of the Bayesian FIM constructed in Section 4. The latter uses the prior knowledge of the targets to predict the range-related information available for target localization over a short prediction horizon, with the objective of maximizing it by proper choice of the inputs to the trackers and, as a consequence, of the tracker trajectories. Only the first term in the optimal sequence of tracker inputs is used to drive the trackers, after which the procedure is repeated.

The MPC scheme is illustrated in Fig. 6.1 and is described as follows. Let $\mathbf{z}_k^{[i]}$ be the state of the tracker i; $i \in \mathcal{S}$ at discrete time k. Assume that at each time instant k the estimates of the targets' states, denoted $\hat{\mathbf{x}}_k^{[\alpha]}$ and their covariance matrices $\hat{P}_k^{[\alpha]} : \alpha \in \mathcal{S}_T$ can be provided by an estimator (e.g. EKF). Given this initial information at time k, the FIM based on N range measurements ahead taken at instants $k+1, \ldots, k+N$ can be predicted using (33) for *Target model A* and (37) for *Target model B*, where N is called the prediction horizon. From (33) and (37), it can be seen that the predicted FIM depends on the trackers' inputs $\mathbf{v}^{[i]}; i \in \mathcal{S}$ and the initial information about the targets. Therefore, the predicted FIM, denoted $\mathcal{I}_p$ is defined explicitly as

$$\mathcal{I}_p(\mathbf{z}_k^{[i]}, \hat{\mathbf{x}}_k^{[\alpha]}, \hat{P}_k^{[\alpha]}, \bar{\mathbf{v}}^{[i]}) \triangleq \begin{cases} \mathcal{I}_{A,N} \text{ for } \textit{Scenario A}, \\ \mathcal{I}_{B,N} \text{ for } \textit{Scenario B}, \end{cases}$$

where $\mathcal{I}_{A,N}$ and $\mathcal{I}_{B,N}$ are computed using (33) and (37), respectively while $\bar{\mathbf{v}}^{[i]} = [[\bar{\mathbf{v}}_k^{[i]}]^T, \ldots, [\bar{\mathbf{v}}_{N-1}^{[i]}]^T]^T; i \in \mathcal{S}$, are the trackers' inputs over the prediction horizon. It is important to note that at every sampled time k, $\mathcal{I}_{A,N}$ and $\mathcal{I}_{B,N}$ are initialized with the prior information $\hat{P}_k^{[\alpha]}$. Based on the discussion in the previous section, the primary objective is to find an optimal input to maximize the range-based information that is defined by the cost

$$J_{\text{FIM}} \triangleq -\log\det\left(\mathcal{I}_p\left(\mathbf{z}_k^{[i]}, \hat{\mathbf{x}}_k^{[\alpha]}, \hat{P}_k^{[\alpha]}, \bar{\mathbf{v}}^{[i]}\right)\right). \tag{55}$$

where $\log\det(\cdot)$ and not simply $\det(\cdot)$ is adopted due to computational advantages [24]. Let $\bar{P}_n^{[\alpha]}; n = k+1, \ldots, k+N$ be the covariance of the target' state predicted over the prediction horizon, computed by using the initial covariance $\hat{P}_k^{[\alpha]}$ and the *Target models (A or B)*. Let $\bar{\lambda}_n^{[\alpha]}$ be the length of the major axis of the ellipse representing the predicted uncertainty region of target's position. Note that $\bar{\lambda}_n^{[\alpha]}$ is computed from $\bar{P}_n^{[\alpha]}$ (for *Target model A*, this is illustrated in Fig. 6.2). For the purpose of ensuring that the trackers pursue the targets and remain in the vicinity of the latter, as stated in task 2 (see Section 3.2), we propose the tracking cost

$$J_{\text{Track}} \triangleq \sum_{i=1}^{p}\sum_{\alpha=1}^{q}\sum_{n=k+1}^{k+N} -\log(r^* - \bar{d}_n^{[i,\alpha]} - \bar{\lambda}_n^{[\alpha]} - \sigma), \tag{56}$$

where $\bar{d}_n^{[i,\alpha]}$ denotes the predicted distance from tracker i to the estimated position of target α, which is computed using (12) over the prediction horizon and r^* is the upper bound for the distance from each tracker to each target.

Let $\bar{\mathbf{e}}^{[i]} = [\bar{v}^{[i]}, \bar{r}^{[i]}]$, where $\bar{v}^{[i]}$ and $\bar{r}^{[i]}$ are the computed linear and angular speeds of the ith tracker, respectively over the prediction horizon. As a means to limit the above values, collectively taken as a proxy for tracker energy consumption, we consider the energy-related cost

$$J_{\text{Energy}} \triangleq \sum_{i=1}^{p}\sum_{n=k}^{k+N-1} \left\|\bar{\mathbf{e}}_n^{[i]}\right\|_{E_i}^2,$$

where $E_i \in \mathbb{R}^{2\times 2}$ is a diagonal matrix and $E_i \succeq 0$ for all $i \in \mathcal{S}$. Finally, to control the smoothness of the linear speed $\bar{v}^{[i]}$ and the angular speed $\bar{r}^{[i]}$ that can be used as references for autopilots on-board the trackers, we define the cost

$$J_{\text{Input}} \triangleq \sum_{i=1}^{p}\sum_{n=k}^{k+N-1} \left\|\bar{\mathbf{v}}_n^{[i]}\right\|_{K_i}^2,$$

where $K_i \succeq 0$ for all $i \in \mathcal{S}$.

With the above ingredients, the problem of computing the trackers' inputs over a given time-horizon with the purpose of yielding good target localization and pursuit can be cast in the form of the following optimal control problem:

Definition 1. The optimal control problem, denoted $\mathcal{OCP}(\mathbf{z}_k^{[i]}, \hat{\mathbf{x}}_k^{[\alpha]}, \hat{P}_k^{[\alpha]}, \bar{\mathbf{v}}^{[i]}(\cdot))$, is stated as follows:

$$\min_{\bar{\mathbf{v}}^{[i]}(\cdot); i\in\mathcal{S}} J_{\text{FIM}} + \rho_1 J_{\text{Track}} + \rho_2 J_{\text{Input}} + \rho_3 J_{\text{Energy}}, \tag{57}$$

subject to

$$\bar{\mathbf{z}}_{n+1}^{[i]} = \mathbf{g}_d(\bar{\mathbf{z}}_n^{[i]}, \bar{\mathbf{v}}_n^{[i]}), \qquad i \in \mathcal{S}, \tag{58a}$$
$$\bar{\mathbf{p}}_n^{[i]} = C\bar{\mathbf{z}}_n^{[i]}, \qquad i \in \mathcal{S}, \tag{58b}$$
$$\bar{\mathbf{z}}_k^{[i]} = \mathbf{z}_k^{[i]}, \qquad i \in \mathcal{S}, \tag{58c}$$
$$\bar{\mathbf{z}}_n^{[i]} \in \mathcal{Z}^{[i]}, \quad \bar{\mathbf{v}}_n^{[i]} \in \mathcal{V}^{[i]}, \qquad i \in \mathcal{S}, \tag{58d}$$
$$\bar{\mathbf{x}}_{n+1}^{[\alpha]} = \mathbf{f}(\bar{\mathbf{x}}_n^{[\alpha]}, \bar{\mathbf{u}}_n^{[\alpha]}), \qquad \alpha \in \mathcal{S}_T, \tag{58e}$$
$$\bar{\mathbf{x}}_k^{[\alpha]} = \hat{\mathbf{x}}_k^{[\alpha]} \qquad \alpha \in \mathcal{S}_T \tag{58f}$$
$$\bar{d}_n^{[i,\alpha]} = \left\|\bar{\mathbf{p}}_n^{[i]} - \bar{\mathbf{q}}_n^{[\alpha]}\right\|, \qquad \alpha \in \mathcal{S}_T, \tag{58g}$$

for $n \in \{k, \ldots, k+N-1\}$, where $\rho_1, \rho_2, \rho_3 \geq 0$ are weighing factors.

In the constraint equations (58), the variables with bar denote predicted variables, to distinguish them from the actual variables, which are without bars. Equations (58a)–(58d) are associated with the trackers' dynamics and the trackers' state and input constraints, while (58e)–(58f) are the constraints associated with

Table 1
Simulation setup.

	Parameters	
Trackers (ASVs)	Depths	$\bar{z}^{[1]} = 0$ m; $\bar{z}^{[2]} = 0$ m
	Velocity constraints	$v^{[i]} \in [0, 4]$ m/s, $r^{[i]} \in [-0.2, 0.2]$ rad/s
	Acceleration constraints	$a_v^{[i]} \in [-0.1, 0.1]$, $a_r^{[i]} \in [-0.01, 0.01]$ for $i \in \{1, 2\}$
Targets (AUVs)	Depth	$\bar{z}_{\mathrm{T}}^{[1]} = 5$ m; $\bar{z}_{\mathrm{T}}^{[2]} = 8$ m
	Velocity vector	$\mathbf{u}^{[\alpha]} = \begin{bmatrix} 0.2 + 0.1\cos(0.1x_{\mathrm{T}}^{[\alpha]}) \\ 0.2 + 0.1\sin(0.1x_{\mathrm{T}}^{[\alpha]}) \end{bmatrix}$ m/s for $\alpha = \{1, 2\}$
	Initial positions	$\mathbf{q}_0^{[1]} = [5, -5]^{\mathrm{T}}$, $\mathbf{q}_0^{[2]} = [0, 0]^{\mathrm{T}}$ m
RMN[a]	Standard deviation	$\sigma = 0.5$ m

[a]Range measurement noise.

the targets' models. Notice how the optimal solution for the trackers' inputs depends on the initial conditions (58c) and (58f) and $\hat{P}_k^{[\alpha]}$; $\alpha \in \mathcal{S}_{\mathrm{T}}$, which are updated at very time k. This implies that the trajectory of the trackers need to be re-planned due to the changes in the initial conditions and justifies our approach of using a receding horizon scheme (MPC) to solve the target localization and pursuit problem. In the MPC scheme, the optimal control problem $\mathcal{OCP}(\cdot)$ is repeatedly solved at every discrete sampling instant k. Let $\bar{\mathbf{v}}^{[i]*}(\cdot)$; $i \in \mathcal{S}$ be the optimal solution of the optimal control problem. The MPC control law for each tracker's input is then defined as

$$\mathbf{v}^{[i]}(t) = \bar{\mathbf{v}}_k^{[i]*} \quad \text{for } t \in [k, k+1) \tag{59}$$

for all $i \in \mathcal{S}$.

In summary, the proposed receding horizon planing, control and estimation for the target localization and pursuit problem can be implemented using Algorithm 1.

Algorithm 1 Receding horizon planing, control and estimation strategy for target localization and pursuit

1: **initialization** ($k = 0$):
2: For target model A: $\hat{\mathbf{x}}_0^{[\alpha]} = \mathbf{c}_{\mathrm{A},0}^{[\alpha]}$, $\hat{P}_0^{[\alpha]} = P_{\mathrm{A},0}^{[\alpha]}$
3: For target model B: $\hat{\mathbf{x}}_0^{[\alpha]} = \mathbf{c}_{\mathrm{B},0}^{[\alpha]}$, $\hat{P}_0^{[\alpha]} = P_{\mathrm{B},0}^{[\alpha]}$
4: At every sampled time k, perform the following procedure:
5: **procedure** Planing, Control and Estimation
6: Solve the $\mathcal{OCP}(\cdot)$ defined by (57) and (58).
7: Collect all ranges from trackers to targets.
8: Run estimators (e.g. EKF) to obtain $\hat{\mathbf{x}}_{k+1}^{[\alpha]}$, $\hat{P}_{k+1}^{[\alpha]}$; $\alpha \in \mathcal{S}_{\mathrm{T}}$
9: **return** $\mathbf{v}^{[i]}$ for all $i \in \mathcal{S}$ using the MPC law (59) and $\hat{\mathbf{x}}_{k+1}^{[\alpha]}$, $\hat{P}_{k+1}^{[\alpha]}$ for all $\alpha \in \mathcal{S}_{\mathrm{T}}$

7. Simulation examples

In this section, we present and discuss simulation results with the objective of illustrating the performance of the proposed MPC framework for localization and pursuit of underwater targets (AUVs) using surface trackers (ASVs). We consider two situations. In the first situation, an ASV is used for single target localization and pursuit, while in the second situation two ASVs are used for localization and pursuit of two targets. The simulation parameters are given in Table 1. Range measurements are available for every $T_s = 2$ s, within the distance of $d_{\max} = 100$ m. Furthermore, the ASVs are required to pursue the AUVs and stay inside each of the AUV's vicinity, with $r^* = 100$ m. The length of the prediction window is set as $N = 6$. To solve the optimal control problem in the MPC scheme, we use Casadi [25], an open source optimization tool. To estimate the target states, an EKF was employed. The design of the EKF is straightforward, thus we omit its description.

Table 2
Prior information on the initial target's state (Gaussian PDF).

	Scenario A[a]	Scenario B[b]
Mean	$\mathbf{c}_{\mathrm{A},0}^{[1]} = [-25, -20]^{\mathrm{T}}$	$\mathbf{c}_{\mathrm{B},0}^{[1]} = [-25, -20, -0, 2, 0, 75]^{\mathrm{T}}$
Cov.	$P_{\mathrm{A},0}^{[1]} = \mathrm{Diag}(200, 200)$	$P_{\mathrm{B},0}^{[1]} = \mathrm{Diag}(200, 200, 0.5, 0.5)$

[a]See (8).
[b]See (11).

To assess the performance of EKF for the localization task, we define the position estimation and velocity estimation errors as follows:

$$\begin{aligned} \mathrm{PosErr} &= \sum_{\alpha=1}^{q} \left\| \mathbf{q}_k^{[\alpha]} - \hat{\mathbf{q}}_k^{[\alpha]} \right\|, \\ \mathrm{VelErr} &= \sum_{\alpha=1}^{q} \left\| \mathbf{u}_k^{[\alpha]} - \hat{\mathbf{u}}_k^{[\alpha]} \right\|, \end{aligned} \tag{60}$$

where $\hat{\mathbf{q}}^{[\alpha]}$ and $\hat{\mathbf{u}}^{[\alpha]}$ are estimated position and velocity vectors of the targets obtained from the EKF, respectively. The simulation results are shown next, while animation videos visualizing the results can be found online at https://doi.org/10.1016/j.robot.2020.103608.

7.1. Simulation 1: Single tracker-single target ($p = 1$, $q = 1$)

In this case, we use one ASV to localize and pursue a single target, that is, $p = q = 1$ and we take the values corresponding to $i = \alpha = 1$ in Table 1. For the MPC scheme, the weighting parameters are set as $\rho_1 = 0.01$ and $\rho_2 = \rho_3 = 0$. The EKF is initialized with the prior information of the target given by Table 2.

The performance of the MPC scheme for target localization and pursuit under with *Scenarios A* and *B* are plotted in Fig. 7.1 and Fig. 7.2, respectively. It can be clearly seen from the figures that the proposed MPC scheme performs well in this simulation set-up. That is, the ASV's trajectories generate "sufficiently rich" range information to estimate the target's state. This can be verified by observing Figs. 7.1(a, b) and 7.2(a, b), where it is evident that the target's state estimation errors converge to a small neighborhood of zero quickly. Comparing Figs. 7.1(a, b) with 7.2(a, b) it can be seen that in *Scenario A*, where the target's velocity vector is known, the estimated target's position converges to the small neighborhood of target's position faster with higher

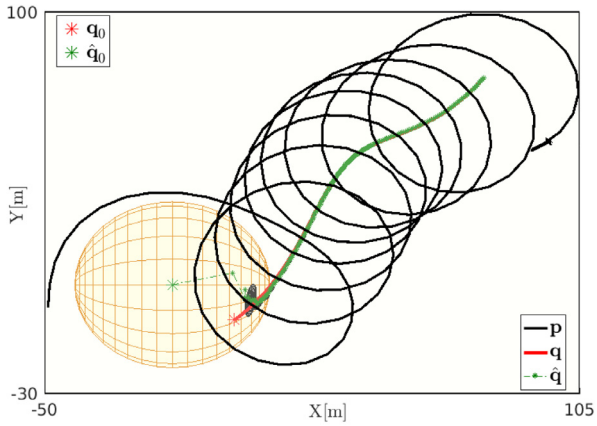

(a) Trajectories projected in 2D: tracker ($\mathbf{p}$), target ($\mathbf{q}$), target estimates ($\hat{\mathbf{q}}$). Ellipses represent the uncertainty region of the estimated target's positions (computed from $\hat{P}_k$) at $k = 0, 10, \ldots, 400$. The brick-red ellipse corresponds to $k = 0$.

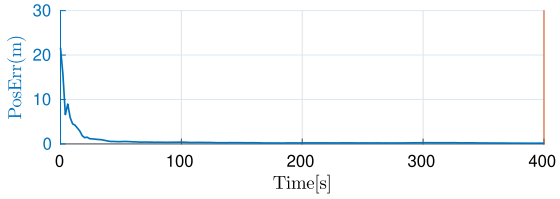

(b) Target's position estimation error

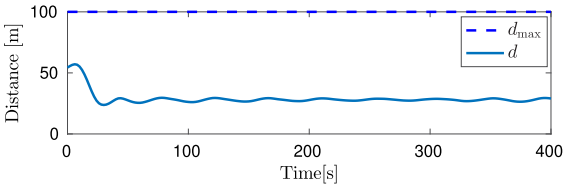

(c) Distance from the tracker to the target

Fig. 7.1. Single tracker-single target for the case where the target's velocity vector is known (*Target model A*).

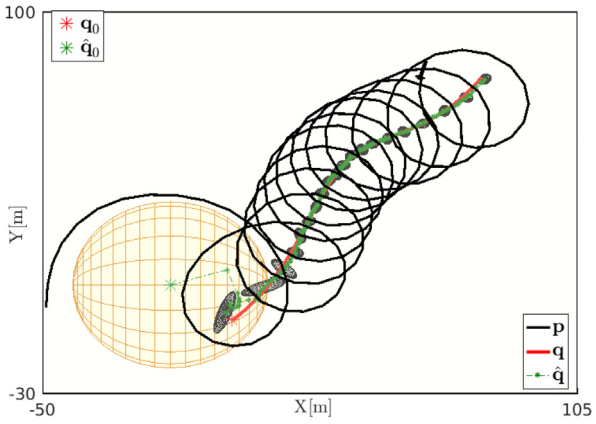

(a) Trajectories projected in 2D: tracker ($\mathbf{p}$), target ($\mathbf{q}$), target estimates ($\hat{\mathbf{q}}$). Ellipses represent the uncertainty region of the estimated target's positions (computed from $\hat{P}_k$) at $k = 0, 10, \ldots, 400$. The brick-red ellipse corresponds to $k = 0$.

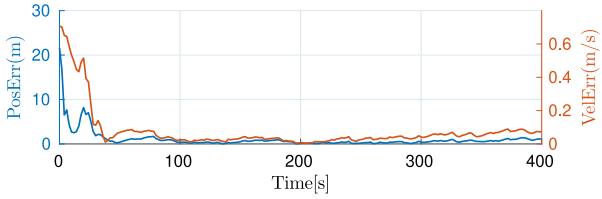

(b) Target's position and velocity estimation errors

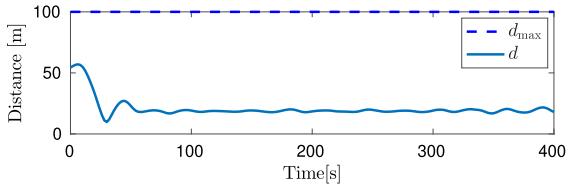

(c) Distance from the tracker to the target

Fig. 7.2. Single tracker-single target for the case where the target's velocity vector is unknown (*Target model B*).

accuracy. Figs. 7.1(c) and 7.2(c) show that the distances from the tracker to the target are kept below r^*, implying that the pursuit task is also fulfilled.

Figs. 7.1(a) and 7.2(a) also show that, regardless of the target model A or B, the ASV follows and encircles the target's uncertainty regions, which are represented by ellipses in the figures. These trajectories are similar to the ideal trajectories stated in Proposition 1 that maximize the range information. Recall that the analysis in Proposition 1 neglected the tracker's constraints and dynamics and the target state is considered to be deterministic. Nevertheless, the analysis provides an intuitive understanding of the trajectories obtained in this simulation when the tracker's constraints and dynamics, and the uncertainty of the target are taken explicitly into account.

7.2. Simulation 2: two trackers - two targets ($p = 2$, $q = 2$)

In this simulation, two trackers (ASVs) are deployed to localize and track two targets. For the MPC scheme, the weighting parameters are set as $\rho_1 = 0.01$, $\rho_2 = 0$, $\rho_3 = 1$, and $E_i = \text{Diag}(0.001, 0.01)$ for $i = \{1, 2\}$. In this simulation, prior information about the initial targets state is used to construct the predicted FIM. The performance of the MPC scheme for target localization and pursuit under *Scenarios A* and *B* are plotted in Fig. 7.3 and Fig. 7.4, respectively. It can be clearly seen in Figs. 7.3(a, b) and 7.4(a, b) that the estimated targets' states quickly converge to the targets' states in both scenarios. It is also interesting to observe from Figs. 7.3(c) and 7.4(c) that the angles between the relative position vectors from the ASVs to each target converge to 90 degree, thus recovering the behavior predicted in Proposition 4 for trajectories that maximize range-information. Figs. 7.3(d) and 7.4(d) show that the distances from the ASVs to the targets are kept smaller than $r^* = 100$ m, thus implying that the pursuit task is fulfilled in both scenarios. Finally, we point out that unlike the case where a single ASV is used, the trajectories of the ASVs are far less demanding in terms of the types of maneuvers.

8. Conclusions

We proposed an optimization-based approach to the problem of multiple target localization and pursuit using measurements of the ranges between the trackers and the targets. The underlying idea of the proposed method is to find optimal trajectories for the trackers that maximize the range-related information embodied in an appropriately defined Bayesian FIM associated with the problem of target state estimation. Analytically, we shown that for the ideal case where the trackers' motion constraints are

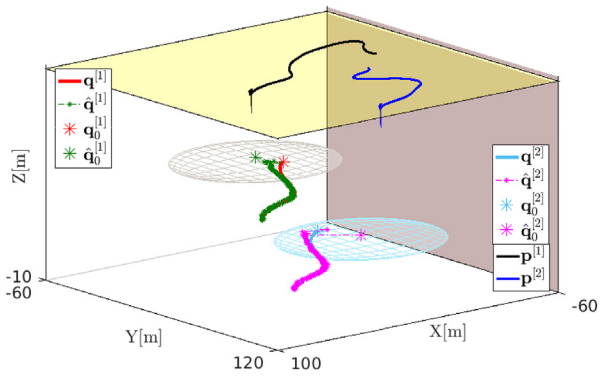

(a) 3D-Trajectories: trackers ($\mathbf{p}^{[i]}$), targets ($\mathbf{q}^{[\alpha]}$), target estimates ($\hat{\mathbf{q}}^{[\alpha]}$); $i, \alpha = 1, 2$. Dark and cyan ellipses describe the uncertainty region in the initial positions of target 1 and 2, respectively.

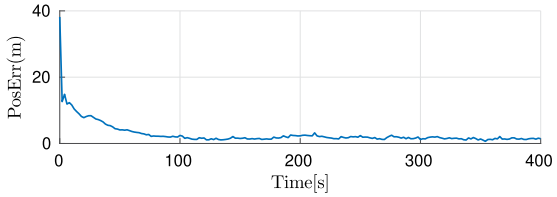

(b) Targets' position estimation error

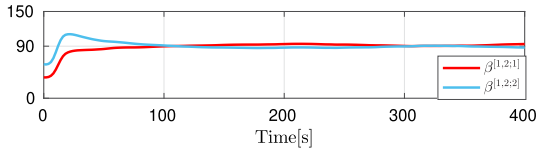

(c) Angles between the relative position vectors from the ASVs to each target (in degrees)

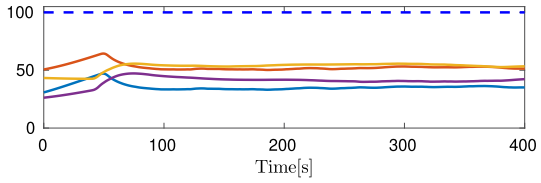

(d) Distances $d^{[i,\alpha]}; i, \alpha = 1, 2$ from the ASVs to the targets (in m). Dash-blue is r^*.

Fig. 7.3. Two trackers and two targets for the case where the targets' velocity vector is known (*Target model A*).

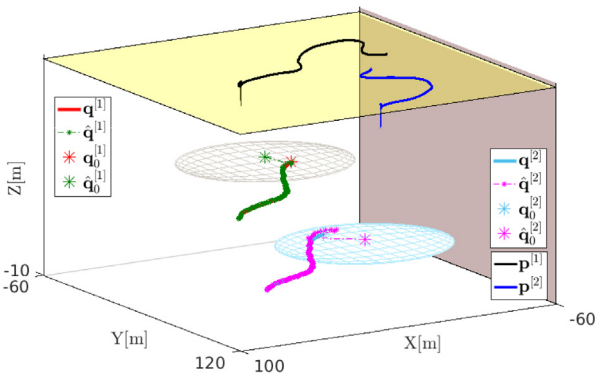

(a) 3D-Trajectories: trackers ($\mathbf{p}^{[i]}$), targets ($\mathbf{q}^{[\alpha]}$), target estimates ($\hat{\mathbf{q}}^{[\alpha]}$); $i, \alpha = 1, 2$. Dark and cyan ellipses describe the uncertainty region in the initial positions of target 1 and 2, respectively.

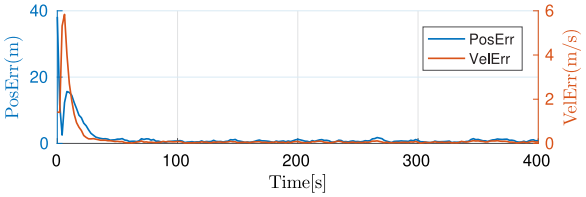

(b) Targets' position velocity estimation errors

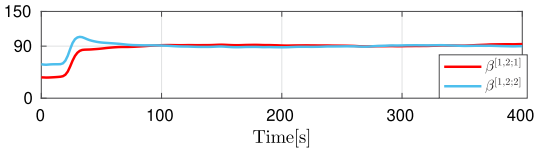

(c) Angles between the relative position vectors from the ASVs to each target (in degrees)

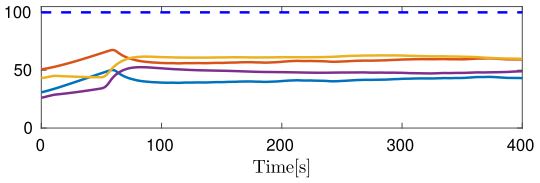

(d) Distances $d^{[i,\alpha]}; i, \alpha = 1, 2$ from the ASVs to the targets (in m). Dash-blue is r^*.

Fig. 7.4. Two trackers and two targets for the case where the targets' velocity vector is unknown (*Target model B*).

neglected and there is no prior information on the initial target's state, there exists an ideal relative geometry of the trackers and the targets for which the range information acquired is maximal. This geometry lends itself to a simple intuitive interpretation. To deal with practical constraints and to consider the fact that the targets' states are random and only estimated on-line, we proposed an MPC framework for optimal tracker motion generation with a view to maximizing the predicted range information for target localization, while taking explicitly into account the trackers' motion constraints, the prior knowledge of the targets' states, and the requirement that the pursuing trackers remain in the vicinities of the targets. By defining appropriate cost and constraints, the MPC scheme is also capable of tackling more challenging cases such as: (i) the trackers must avoid obstacles and (ii) collision avoidance between the trackers. Future work will aim at decentralizing the MPC scheme, and implementing it in a distributed manner, making the proposed method more scalable for the case where a larger numbers of trackers may be used.

Declaration of competing interest

The authors declare that they have no known competing financial interests or personal relationships that could have appeared to influence the work reported in this paper.

Appendix A. Proofs of Theorems and Propositions

The following lemmas will be used in the proof:

Lemma 2. *Let* $U, V \in \mathbb{R}^{n\times n}$ *and* $U, V \succeq 0$. *Then,* $\det(U)+\det(V) \leq \det(U+V)$.

The lemma follows from Minkowski's determinant inequality (see [26], p. 510).

Lemma 3. *If the trackers and the targets operate at the same depth, that is, $\bar{z}^{[i]} = \bar{z}_{\mathrm{T}}^{[\alpha]}$ for all $i \in S, \alpha \in \mathcal{S}_{\mathrm{T}}$, then $a_n^{[i,\alpha]} = \cos(\gamma_n^{[i,\alpha]})$ and $b_n^{[i,\alpha]} = \sin(\gamma_n^{[i,\alpha]})$ for all $i \in \mathcal{S}, \alpha \in \mathcal{S}_{\mathrm{T}}$ and $n \in \{1, \ldots, k\}$.*

The lemma follows directly from (12), (38), and (43).

A.1. Proof of Theorem 1

i. We first prove the result for *Scenario A*. In this case, $i = p = 1$ and $\alpha = q = 1$. Thus, (39) can be rewritten as

$$\mathcal{I}_{\mathrm{A},k} = \frac{1}{\sigma^2}\begin{bmatrix} \|\mathbf{a}\|^2 & \mathbf{a}^{\mathrm{T}}\mathbf{b} \\ \mathbf{a}^{\mathrm{T}}\mathbf{b} & \|\mathbf{b}\|^2 \end{bmatrix}. \tag{61}$$

Recall that in this simple case we dropped the superscript (subscript) α in (39) for simplicity in notation. We define $z_n = (\bar{z} - \bar{z}_{\mathrm{T}})^2/d_n^2$ for all $n \in \{1, \ldots, k\}$. It follows from (42) and Assumption 1 that

$$z_n \geq c \tag{62}$$

for all n. Let

$$\mathbf{z} = [z_1, \ldots, z_k]^{\mathrm{T}} \in \mathbb{R}^k \tag{63}$$

and define

$$Z_{\mathrm{A}} = \sigma^{-2}\mathrm{Diag}(\|\mathbf{z}\|^2/2, \|\mathbf{z}\|^2/2). \tag{64}$$

Because of (62), it can be seen that

$$\det(Z_{\mathrm{A}}) \geq \det(Z_{\mathrm{A}}^*) \tag{65}$$

for all $\mathbf{z}$, where $Z_{\mathrm{A}}^* \triangleq c\sigma^{-2}I_2 k/2 = c\sigma^{-2}\mathcal{I}_{\mathrm{A}}^o$. The equality holds when $Z_{\mathrm{A}} = Z_{\mathrm{A}}^*$, that is, when $z_n = c$ for all $n \in \{1, \ldots, k\}$. We now consider the matrix

$$X \triangleq \mathcal{I}_{\mathrm{A},k} + Z_A = \frac{1}{\sigma^2}\begin{bmatrix} \|\mathbf{a}\|^2 + \|\mathbf{z}\|^2/2 & \mathbf{a}^{\mathrm{T}}\mathbf{b} \\ \mathbf{a}^{\mathrm{T}}\mathbf{b} & \|\mathbf{b}\|^2 + \|\mathbf{z}\|^2/2 \end{bmatrix}. \tag{66}$$

By definition, X is symmetric and has a constant trace, that is, $\mathrm{Tr}(X) = \sigma^{-2}(\|\mathbf{a}\|^2 + \|\mathbf{b}\|^2 + \|\mathbf{z}\|^2) = \sigma^{-2}k$ for all $\mathbf{a}$, $\mathbf{b}$ and $\mathbf{z}$. Using Theorem 1.2 in [27] it follows that

$$\det(X) \leq \det(X^*), \tag{67}$$

for all $\mathbf{a}$, $\mathbf{b}$ and $\mathbf{z}$, where $X^* \triangleq \sigma^{-2}\mathrm{Diag}(k/2, k/2) = \sigma^{-2}\mathcal{I}_{\mathrm{A}}^o$. The equality holds when $X = X^*$. Because $\mathcal{I}_{\mathrm{A},k}, Z_{\mathrm{A}} \succeq 0$, it follows from Lemma 1 and (65)–(67) that $\det(\mathcal{I}_{\mathrm{A},k}) \leq \det(X) - \det(Z_{\mathrm{A}}) \leq \det(X^*) - \det(Z_{\mathrm{A}}^*)$. The equality holds when $X = X^*$ and $Z = Z_{\mathrm{A}}^*$. In other words, $\det(\mathcal{I}_{\mathrm{A},k})$ is maximal when $\mathcal{I}_{\mathrm{A},k} = X^* - Z_{\mathrm{A}}^* = (1-k)\sigma^{-2}\mathcal{I}_{\mathrm{A}}^o = \mathcal{I}_{11\mathrm{A}}$. This concludes the proof for *Scenario A*.

ii. We now present the proof for *Scenario B*. To this end, define

$$Z = \begin{bmatrix} Z_{\mathrm{A}} & Z_{\mathrm{B}} \\ Z_{\mathrm{B}} & Z_{\mathrm{C}} \end{bmatrix} \in \mathbb{R}^{4\times 4}, \tag{68}$$

where Z_{A} is given by (64) and

$$\begin{aligned} Z_{\mathrm{B}} &= -\sigma^{-2}\mathrm{Diag}(\|\mathbf{z}\|_{D_1}^2/2, \|\mathbf{z}\|_{D_1}^2/2), \\ Z_{\mathrm{C}} &= \sigma^{-2}\mathrm{Diag}(\|\mathbf{z}\|_{D_2}^2/2, \|\mathbf{z}\|_{D_2}^2/2), \end{aligned} \tag{69}$$

with $\mathbf{z}$ is as in (63). We now consider the matrix

$$Y \triangleq \mathcal{I}_{\mathrm{B},k} + Z = \begin{bmatrix} A + Z_{\mathrm{A}} & B + Z_{\mathrm{B}} \\ B + Z_{\mathrm{B}} & C + Z_{\mathrm{C}} \end{bmatrix} \triangleq \begin{bmatrix} Y_{\mathrm{A}} & Y_{\mathrm{B}} \\ Y_{\mathrm{B}} & Y_{\mathrm{C}} \end{bmatrix},$$

where A, B, C are given by (41). To show that $\det(\mathcal{I}_{\mathrm{B},k})$ is maximal when $\mathcal{I}_{\mathrm{B},k} = \mathcal{I}_{11\mathrm{B}}$, we assume that the following hypotheses hold true (this will be shown later).

- *Hypothesis 1*: $\det(Z) \geq \det(Z^*)$ for all $\mathbf{z}$, where $Z^* = c\sigma^{-2}\mathcal{I}_{\mathrm{B}}^o$. The equality holds when $Z = Z^*$.
- *Hypothesis 2*: $\det(Y) \leq \det(Y^*)$ for all $\mathbf{a}, \mathbf{b}$ and $\mathbf{z}$, where $Y^* = \sigma^{-2}\mathcal{I}_{\mathrm{B}}^o$. The equality holds when $Y = Y^*$.

Using the hypotheses and arguments similar to those presented for *Scenario A*, we can show that $\det(\mathcal{I}_{\mathrm{B},k})$ is maximal when $\mathcal{I}_{\mathrm{B},k} = Y^* - Z^* = (1-c)\sigma^{-2}\mathcal{I}_{\mathrm{B}}^o = \mathcal{I}_{11\mathrm{B}}$. To complete the proof for *Scenario B* we prove the hypotheses above as follows.

Proof of Hypothesis 1. If $\bar{z} = \bar{z}_{\mathrm{T}}$, it follows that $Z = Z^* = 0$. Thus, *Hypothesis 1* holds trivially. Now consider the case $\bar{z} \neq \bar{z}_{\mathrm{T}}$. This implies that $Z_{\mathrm{A}} \succ 0$. Using the Schur's complement of matrix Z yields

$$\det(Z) = \det(Z_{\mathrm{A}})\det(Z_{\mathrm{C}} - Z_{\mathrm{B}}Z_{\mathrm{A}}^{-1}Z_{\mathrm{B}}). \tag{70}$$

From (69), we obtain

$$Z_{\mathrm{C}} - Z_{\mathrm{B}}Z_{\mathrm{A}}^{-1}Z_{\mathrm{B}} = \sigma^{-2}\mathrm{Diag}(\lambda/2, \lambda/2), \tag{71}$$

where $\lambda = \|\mathbf{z}\|_{D_2}^2 - (\|\mathbf{z}\|_{D_1}^2)^2/\|\mathbf{z}\|^2$. Expanding λ yields

$$\begin{aligned} \lambda\|\mathbf{z}\|^2 &= \left(\sum_{n=1}^k z_n^2\tau_n^2\right)\left(\sum_{n=1}^k z_n^2\right) - \left(\sum_{n=1}^k z_n^2\tau_n\right)^2 \\ &= \underbrace{\frac{1}{2}\sum_{i,j=1}^k z_i^2 z_j^2(\tau_i - \tau_j)^2}_{\triangleq M} > 0. \end{aligned}$$

From (64), (70), and (71) it follows that

$$\det(Z) = \left(\frac{\sigma^{-4}\|\mathbf{z}\|^4}{4}\right)\left(\frac{\sigma^{-4}\lambda^2}{4}\right) = \frac{\sigma^{-8}}{16}M^2 > 0.$$

It can be easily seen that when the sampling interval is fixed, that is τ_n, $n \in \{1, \ldots, k\}$ is constant, then M is lower bounded by the lower bound of z_n for $n \in \{1, \ldots, k\}$. Because of (62), $\det(Z)$ is minimum when $z_n = c$. Substituting $z_n = c$ for all $n \in \{1, \ldots, k\}$ in (68) we conclude that $\det(Z)$ is minimum at $Z = c\sigma^{-2}\mathcal{I}_{\mathrm{B}}^o = Z^*$.

Proof of Hypothesis 2. Consider the matrix Y. It can be checked that the trace of each block of Y is always constant. Specifically, $\mathrm{Tr}(Y_{\mathrm{A}}) = \mathrm{Tr}(A + Z_{\mathrm{A}}) = \|\mathbf{a}\|^2 + \|\mathbf{b}\|^2 + \|\mathbf{z}\|^2 = k/\sigma^2$. Similarly, $\mathrm{Tr}(Y_{\mathrm{B}}) = \mathrm{Tr}(B + Z_{\mathrm{B}}) = \Delta_1/\sigma^2$ and $\mathrm{Tr}(Y_{\mathrm{C}}) = \mathrm{Tr}(C + Z_{\mathrm{C}}) = \Delta_2/\sigma^2$. Applying Theorem 1.2 in [27] it follows that $\det(Y)$ is maximized if and only if each block is a scaled identity matrix of the form $Y_{\mathrm{A}} = \mathrm{Tr}(Y_{\mathrm{A}})I_2/2 = \sigma^{-2}kI_2/2$, $Y_{\mathrm{B}} = \mathrm{Tr}(Y_{\mathrm{B}})I_2/2 = \sigma^{-2}\Delta_1 I_2/2$ and $Y_{\mathrm{C}} = \mathrm{Tr}(Y_{\mathrm{C}})I_2/2 = \sigma^{-2}\Delta_2 I_2/2$. Comparing with (47), this proves *Hypothesis 2*, thus completing the proof for *Scenario B* and Theorem 1. ■

A.2. Proof of Proposition 1

The proof is done for Scenario A. The proof for Scenario B is identical. Theorem 1 implies that the range information is maximal when $\mathcal{I}_{\mathrm{A},k} = \mathcal{I}_{11\mathrm{A}}$. This, together with (44), (45) and (61) implies that

$$\|\mathbf{a}\|^2 = \|\mathbf{b}\|^2 = (1-c)k/2, \tag{72a}$$

$$\mathbf{a}^{\mathrm{T}}\mathbf{b} = 0. \tag{72b}$$

We now show that the tracker's trajectory stated in Proposition 1 satisfies (72).

i. We first consider the case where the tracker and the target are at the same depth, that is, $z = z_{\mathrm{T}}$ and therefore $c = 0$. Using Lemma 3, (72) can be rewritten as

$$\sum_{n=1}^k \cos^2(\gamma_n) = \sum_{n=1}^k \sin^2(\gamma_n) = k/2, \tag{73a}$$

$$\sum_{n=1}^k \cos(\gamma_n)\sin(\gamma_n) = 0. \tag{73b}$$

For $k \geq 3$, it is well-known that in order to satisfy (73) the angle displacement between any two successive angles must be equal and satisfy $(\gamma_{n+1}-\gamma_n)k = 2\pi l$, where $l = 1, 2, \ldots$, see [6,7]. If the tracker can actually move so that (48) is satisfied, then at discrete time instants $k = 2\pi l/\omega = Nl$, $\mathcal{I}_{\mathrm{A},k} = \mathcal{I}_{11\mathrm{A}}$, where $l = 1, 2, \ldots$.

ii. We now consider the case where the tracker and the target are at different depths. A solution to (72a) is $a_n^2 + b_n^2 = 1 - c$ for all $n \in \{1, \ldots, k\}$. Further, as shown in the proof of Theorem 1, in order to obtain the maximal range information, $d_n = d_{\max}$ for all $n \in \{1, \ldots, k\}$. Hence, it follows from (38) that the trajectory of the tracker must satisfy $(x_n - x_{\mathrm{T},n})^2 + (y_n - y_{\mathrm{T},n})^2 = d_{\max}^2 - (z - z_{\mathrm{T}})^2$ for all $n \in \{1, \ldots, k\}$. This implies that the tracker must encircle the target with a radius $r \triangleq \sqrt{d_{\max}^2 - (z - z_{\mathrm{T}})^2}$. This completes the proof. ■

A.3. Proof of Theorem 2

i. We first consider *Scenario A*. To this end, let

$$z_n^{[i,\alpha]} = (\bar{z}^{[i]} - \bar{z}_{\mathrm{T}}^{[\alpha]})^2/(d_n^{[i,\alpha]})^2 \tag{74}$$

and define the vector $\mathbf{z}^{[i,\alpha]} = [z_1^{[i,\alpha]}, \ldots, z_k^{[i,\alpha]}]^{\mathrm{T}} \in \mathbb{R}^k$. Define also the matrix

$$Z_\alpha = \sum_{i=1}^{p} \frac{1}{\sigma^2} \begin{bmatrix} \left\|\mathbf{z}^{[i,\alpha]}\right\|^2/2 & 0 \\ 0 & \left\|\mathbf{z}^{[i,\alpha]}\right\|^2/2 \end{bmatrix}.$$

Consider now the matrix $F \triangleq \mathcal{I}_{\mathrm{A},k}^{[\alpha]} + Z_\alpha$, where $\mathcal{I}_{\mathrm{A},k}^{[\alpha]}$ given by (39). It can be checked that F has a constant trace, that is, $\mathrm{Tr}(F) = \sum_{i=1}^{p}(\left\|\mathbf{a}_{i,\alpha}\right\|^2 + \left\|\mathbf{b}_{i,\alpha}\right\|^2 + \left\|\mathbf{z}^{[i,\alpha]}\right\|^2) = \sum_{i=1}^{p}\sigma^{-2}k = p\sigma^{-2}k$. Using Theorem 1.2 in [27], we conclude that $\det(F)$ is maximal when $F = F^* \triangleq p\sigma^{-2}kI_2/2 = p\sigma^{-2}\mathcal{I}_{\mathrm{A}}^o$. Furthermore, because $z_n^{[i,\alpha]} \geq c^{[i,\alpha]}$ for all $d_n^{[i,\alpha]}$ it is obvious that $\det(Z_\alpha)$ is minimum when $Z_\alpha = Z_\alpha^* \triangleq \sum_{i=1}^{p} c^{[i,\alpha]}\sigma^{-2}\mathcal{I}_{\mathrm{A}}^o$. Similar to the proof of Theorem 1 for *Scenario A*, we conclude that $\det(\mathcal{I}_{\mathrm{A},k}^{[\alpha]})$ is maximal when $\mathcal{I}_{\mathrm{A},k}^{[\alpha]} = F^* - Z_\alpha^* = \bar{\mathcal{I}}_{\mathrm{A},k}^{[\alpha]}$. This concludes the proof for *Scenario A*.

ii. The proof for *Scenario B* follows using the methodology adopted in the proof for *Scenario A*. ■

A.4. Proof of Proposition 2

We prove this proposition by showing that the conditions on the trackers' trajectories given in Proposition 2 yield the optimal range information matrices introduced in Theorem 2 for the case of two trackers ($p = 2$) and a single target. The proof is done for *Scenario A*, the methodology adopted carrying over to the proof of *Scenario B*.

Theorem 2 implies that in order to maximize the range information, one must have $\mathcal{I}_{\mathrm{A},k}^{[\alpha]} = \bar{\mathcal{I}}_{\mathrm{A},k}^{[\alpha]}$. From (39) and (49), this implies that

$$\sum_{i=1}^{2} \frac{1}{\sigma^2} \begin{bmatrix} \left\|\mathbf{a}_{i,\alpha}\right\|^2 & \mathbf{a}_{i,\alpha}^{\mathrm{T}}\mathbf{b}_{i,\alpha} \\ \mathbf{a}_{i,\alpha}^{\mathrm{T}}\mathbf{b}_{i,\alpha} & \left\|\mathbf{b}_{i,\alpha}\right\|^2 \end{bmatrix} = \left(2 - \sum_{i=1}^{2} c^{[i,\alpha]}\right)\sigma^{-2}\mathcal{I}_{\mathrm{A}}^o. \tag{75}$$

Eq. (75) is equivalent to

$$\sum_{i=1}^{2} \left\|\mathbf{a}_{i,\alpha}^2\right\| = \sum_{i=1}^{2} \left\|\mathbf{b}_{i,\alpha}\right\|^2 = (2 - \sum_{i=1}^{2} c^{[i,\alpha]})k/2, \tag{76a}$$

$$\sum_{i=1}^{2} \mathbf{a}_{i,\alpha}^{\mathrm{T}}\mathbf{b}_{i,\alpha} = 0 \tag{76b}$$

i. We start by considering the case when the trackers and the target are at the same depth, that is, $\bar{z}^{[i]} = \bar{z}^{[\alpha]}$ for all $i \in \{1, 2\}$. Using Lemma 3, (76b) can be rewritten as

$$\sum_{n=1}^{k} \cos(\gamma_n^{[1,\alpha]})\sin(\gamma_n^{[1,\alpha]}) + \cos(\gamma_n^{[2,\alpha]})\sin(\gamma_n^{[2,\alpha]}) = 0 \tag{77}$$

for all $n \in \{1, \ldots, k\}$. It can be easily checked that $\beta_n^{[1,2;\alpha]} \triangleq \gamma_n^{[1,\alpha]} - \gamma_n^{[2,\alpha]} = \pi/2 + l\pi$ for all $n \in \{1, \ldots, k\}$ and $l \in \mathbb{Z}$ satisfies (77). This concludes the case where the trackers and the target are at the same depth.

ii. We now consider the case when the trackers and the target are at different depths. A solution to (76a) is $(a_n^{[i,\alpha]})^2 + (b_n^{[i,\alpha]})^2 = 1 - c^{[i,\alpha]}$ for all $n \in \{1, \ldots, k\}$. Further, as shown in the proof of Theorem 2, $d_n^{[i,\alpha]} = d_{\max}$ for all $i \in \mathcal{S}$ and $n \in \{1, \ldots, k\}$ in order to obtain the maximal range information. Hence, it follows from (38) that the trajectory of the trackers must satisfy $\left\|\mathbf{p}_n^{[i]} - \mathbf{q}_n^{[\alpha]}\right\| = \sqrt{d_{\max}^2 - (z^{[i]} - z_{\mathrm{T}}^{[\alpha]})^2}$ for all $i \in \{1, 2\}$ and $n \in \{1, \ldots, k\}$. This completes the proof. ■

A.5. Proof of Proposition 3

i. For the cases where the trackers and the targets have the same depth, the proof can be found in Proposition 3 in [6].

ii. If the depths are different, the proof can be done analogously. ■

A.6. Proof of Theorem 3

i. For *Scenario A*, from (33) it follows that $\det(\mathcal{I}_{\mathrm{A},k}) = \prod_{\alpha=1}^{q} \det(\mathcal{I}_{\mathrm{A},k}^{[\alpha]})$. Hence, $\det(\mathcal{I}_{\mathrm{A},k})$ is maximal when each $\det(\mathcal{I}_{\mathrm{A},k}^{[\alpha]})$; $\alpha \in \{1, \ldots, q\}$ is maximal. In Theorem 2, it was shown that for each α, $\det(\mathcal{I}_{\mathrm{A},k}^{[\alpha]})$ is maximal when $\mathcal{I}_{\mathrm{A},k}^{[\alpha]} = \bar{\mathcal{I}}_{\mathrm{A},k}^{[\alpha]}$ for all $\alpha \in \{1, \ldots, q\}$. This implies that $\det(\mathcal{I}_{\mathrm{A},k})$ is maximal when $\mathcal{I}_{\mathrm{A},k} = \mathrm{Diag}(\bar{\mathcal{I}}_{\mathrm{A},k}^{[1]}, \ldots, \bar{\mathcal{I}}_{\mathrm{A},k}^{[q]})$. This concludes the proof for *Scenario A*.

ii. The proof for *Scenario B* follows similar arguments. ■

Appendix B. Supplementary data

Supplementary material related to this article can be found online at https://doi.org/10.1016/j.robot.2020.103608.

References

[1] C.M. Clark, C. Forney, E. Manii, D. Shinzaki, C. Gage, M. Farris, C.G. Lowe, M. Moline, Tracking and following a tagged leopard shark with an autonomous underwater vehicle, J. Field Robotics 30 (3) (2013) 309–322.

[2] A. Zolich, T.A. Johansen, J.A. Alfredsen, J. Kuttenkeuler, E. Erstorp, A formation of unmanned vehicles for tracking of an acoustic fish-tag, in: OCEANS 2017, Anchorage, 2017, pp. 1–6.

[3] L. Philippe, H. Jean-Philippe, M. Jean-Claude, N. Eric, Air and Spaceborne Radar Systems: An Introduction, William Andrew Publishing, Norwich, NY, 2001.

[4] B. Ristic, S. Arulampalam, N. Gordon, Beyond the Kalman Filter, Artech House, 2004.

[5] S. Martinez, F. Bullo, Optimal sensor placement and motion coordination for target tracking, Automatica 42 (4) (2006) 661–668, http://dx.doi.org/10.1016/j.automatica.2005.12.018, URL http://www.sciencedirect.com/science/article/pii/S000510980600015X.

[6] A.N. Bishop, B. Fidan, B.D.O. Anderson, K. Dogancay, P.N. Pathirana, Optimality analysis of sensor-target localization geometries, Automatica 46 (3) (2010) 479–492.

[7] D. Moreno-Salinas, A.M. Pascoal, J. Aranda, Optimal sensor placement for multiple target positioning with range-only measurements in two-dimensional scenarios, Sensors 13 (8) (2013) 10674–10710.

[8] D. Moreno-Salinas, A. Pascoal, J. Aranda, Optimal sensor placement for acoustic underwater target positioning with range-only measurements, IEEE J. Ocean. Eng. 41 (3) (2016) 620–643, http://dx.doi.org/10.1109/JOE.2015.2494918.

[9] I. Masmitja, S. Gomariz, J. Del-Rio, B. Kieft, T. O'Reilly, P. J Bouvet, J. Aguzzi, Optimal path shape for range-only underwater target localization using a Wave Glider, Int. J. Robot. Res. 37 (12) (2018) 1447–1462.
[10] I. Masmitja, P.J. Bouvet, S. Gomariz, J. Aguzzi, J. del Rio, Underwater mobile target tracking with particle filter using an autonomous vehicle, in: OCEANS 2017, Aberdeen, 2017, pp. 1–5.
[11] F. Mandić, I. Rendulić, N. Mišković, N. Dula, Underwater object tracking using sonar and USBL measurements, J. Sens. 2016 (2016).
[12] G. Indiveri, P. Pedone, M. Cuccovillo, Fixed target 3D localization based on range data only: A recursive least squares approach, IFAC Proc. Vol. 45 (5) (2012) 140–145, 3rd IFAC Workshop on Navigation, Guidance and Control of Underwater Vehicles.
[13] N. Crasta, D. Moreno-Salinas, A.M. Pascoal, J. Aranda, Multiple autonomous surface vehicle motion planning for cooperative range-based underwater target localization, Annu. Rev. Control 46 (2018) 326–342.
[14] D. Pillon, A. Perez-Pignol, C. Jauffret, Observability: range-only versus bearings-only target motion analysis for a leg-by-leg observer's trajectory, IEEE Trans. Aerosp. Electron. Syst. 52 (4) (2016) 1667–1678.
[15] C. Jauffret, A. Pérez, D. Pillon, Observability: Range-only versus bearings-only target motion analysis when the observer maneuvers smoothly, IEEE Trans. Aerosp. Electron. Syst. 53 (6) (2017) 2814–2832.
[16] F. Arrichiello, G. Antonelli, A. Aguiar, A. Pascoal, An observability metric for underwater vehicle localization using range measurements, Sensors 13 (12) (2013) 16191–16215.
[17] Nguyen T. Hung, António M. Pascoal, Range-based navigation and target localization-observability analysis and guidelines for motion planning, in: 21st IFAC World Congress, 2020, https://www.dropbox.com/s/90u31vku7omcrbc/IFAC2020.pdf?dl=0, in press.
[18] R. Hermann, A. Krener, Nonlinear controllability and observability, IEEE Trans. Automat. Control 22 (5) (1977) 728–740.
[19] P. Tichavsky, C.H. Muravchik, A. Nehorai, Posterior Cramer-Rao bounds for discrete-time nonlinear filtering, IEEE Trans. Signal Process. 46 (5) (1998) 1386–1396, http://dx.doi.org/10.1109/78.668800.
[20] H.L. Van Trees, Part I: Detection, estimation, and linear modulation theory, Wiley, 1968.
[21] B. Ristic, S. Arulampalam, J. McCarthy, Target motion analysis using range-only measurements: Algorithms, performance and application to ISAR data, Signal Process. 82 (2) (2002) 273–296.
[22] I. Masmitja, S. Gomariz, J. Del-Rio, B. Kieft, T. O'Reilly, P. Bouvet, J. Aguzzi, Range-only single-beacon tracking of underwater targets from an autonomous vehicle: From theory to practice, IEEE Access 7 (2019) 86946–86963, http://dx.doi.org/10.1109/ACCESS.2019.2924722.
[23] Francisco C. Rego, Nguyen T. Hung, Colin N. Jones, Antonio M. Pascoal, A. Pedro Aguiar, Cooperative path-following control with logic-based communications: theory and practice, in: Navigation and Control of Autonomous Marine Vehicles, IET, 2019, http://dx.doi.org/10.1049/PBTR011E.
[24] Stephen Boyd, Lieven Vandenberghe, Convex Optimization, Cambridge University Press, 2004.
[25] J. Andersson, A General-Purpose Software Framework for Dynamic Optimization, Arenberg Doctoral School, KU Leuven, 2013.
[26] R.A. Horn, C.R. Johnson, Matrix Analysis, Second ed., Cambridge University Press, 2012.
[27] O. Popescu, C. Rose, D.C. Popescu, Maximizing the determinant for a special class of block-partitioned matrices, Math. Probl. Eng. 2004 (1) (2004) 49–61.

Nguyen T. Hung received the B.E. and M.Sc. degrees in electrical and electronics engineering form the Ho Chi Minh City University of Technology, Viet Nam and the University Technology Petronas, Malaysia in 2010 and 2015, respectively. He was a research fellow with the Marie Sklodowska Curie Innovative Training Networks of the MarineUAS project from 2016–2018. He is currently pursing a Ph.D. degree at the Institute for Systems and Robotics, Instituto Superior Tecnico, University of Lisbon, Portugal. His research interests include control, estimation, optimization, and network science with applications in aerial and marine robots.

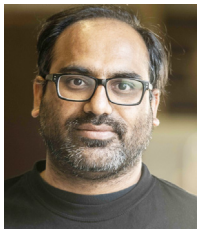

Naveen Crasta received the B.E. degree in electrical and electronics engineering from the Manipal Institute of Technology, Manipal, India, in 2000, the M.Tech. degree in control and automation from the Indian Institute of Technology, Delhi, in 2004, and the Ph.D. degree in aerospace engineering from the Indian Institute of Technology, Bombay, in 2009. He is currently a researcher with the Institute for Systems and Robotics, Superior Técnico, University of Lisbon, Lisbon, Portugal. His interests include nonlinear systems theory, dynamics and control of rotational motion, estimation theory, and marine robotics.

David Moreno-Salinas received the Degree of Engineer in industrial electronics and the Degree of Engineer in automatic control and electronics from the University of Cordoba, Córdoba, Spain, in 2003 and 2006, respectively, and the Ph.D. degree in computer science from the National University Distance Education (UNED), Madrid, Spain, in 2013. He worked for the Agency of R+D of the regional government of Andalucia (2006–2007). From 2007, he was with the Department of Computer Science and Automatic Control, UNED, as a Ph.D. student, and in 2010, he became an Assistant Professor. His scientific activities cover aspects from estimation, positioning, sensor networks, modeling and simulation, and control and robotics.

António M. Pascoal received the Ph.D. degree in Control Science from the Univ. Minnesota, Mpls, USA in 1987. Since 1988 he has been with the Department of Electrical Engineering of the Instituto Superior Tecnico (IST), Univ. Lisbon, PT where he lectures in the areas of Control and Robotics. From 1996–1998 he was a Visiting Associate Professor with the Department of Aeronautics and Astronautics of the US Naval Postgraduate School of Monterey, California, USA. He is currently an Associate Professor of IST, a senior researcher with the Institute for Systems and Robotics (ISR), and coordinator of the Thematic Area "Technologies for Ocean Exploration and Exploitation" of the Laboratory of Robotics and Engineering Systems (LARSyS). Since 2012, he has been an Adjunct Scientist with the National Institute of Oceanography, Goa, India. He was elected Chair, IFAC Technical Committee Marine Systems, from 2008–2014. He has coordinated and participated in a large number of international projects that have led to the design, development, and field-testing of single and multiple autonomous marine and air vehicles in cooperation with partners in India (National Institute of Oceanography, Goa), USA (Naval Postgraduate School, Monterey, CA), Korea (KAIST), and Europe. His research interests include Dynamical Systems Theory and Robotics with applications to the development of aerial and marine robots for ocean exploration and exploitation.

Tor Arne Johansen received the M.Sc. And Ph.D. degrees in electrical and computer engineering from the Norwegian University of Science and Technology (NTNU), Trondheim, Norway, in 1989 and 1994, respectively. From 1995 to 1997, he was with SINTEF as a Researcher, and later he was appointed as an Associated Professor at NTNU in 1997 and a Professor in 2001. In 2002, he cofounded the company Marine Cybernetics AS, where he was the Vice President until 2008. He has authored/coauthored several hundred articles in the areas of control, estimation, and optimization with applications in the marine, aerospace, automotive, biomedical, and process industries. Prof. Johansen received the 2006 Arch T. Colwell Merit Award of the SAE, and he is currently a Principal Researcher within the Center of Excellence on Autonomous Marine Operations and Systems and the Director of the Unmanned Aerial Vehicle Laboratory at NTNU.